The James Webb Space Telescope mission

Gardner, J.P.; Mather, J.C.; Abbott, R.; Abell, J.S.; Abernathy, M.; Abney, F.E.; ... ; et al.

Publications of the Astronomical Society of the Pacific, 135:068001 (24pp), 2023 June https://doi.org/10.1088/1538-3873/acd1b5

The James Webb Space Telescope Mission

Jonathan P. Gardner[1], John C. Mather[1], Randy Abbott[2,87], James S. Abell[1], Mark Abernathy[3], Faith E. Abney[3], John G. Abraham[1], Roberto Abraham[4,5], Yasin M. Abul-Huda[3], Scott Acton[2], Cynthia K. Adams[1], Evan Adams[3], David S. Adler[3], Maarten Adriaensen[6], Jonathan Albert Aguilar[3], Mansoor Ahmed[1,87], Nasif S. Ahmed[3], Tanjira Ahmed[1], Rüdeger Albat[6], Loïc Albert[7], Stacey Alberts[8], David Aldridge[9], Mary Marsha Allen[3], Shaune S. Allen[1], Martin Altenburg[10], Serhat Altunc[1], Jose Lorenzo Alvarez[11], Javier Álvarez-Márquez[12], Catarina Alves de Oliveira[13], Leslie L. Ambrose[1], Satya M. Anandakrishnan[14], Gregory C. Andersen[1], Harry James Anderson[3], Jay Anderson[3], Kristen Anderson[14], Sara M. Anderson[3], Julio Aprea[6], Benita J. Archer[1], Jonathan W. Arenberg[14], Ioannis Argyriou[15], Santiago Arribas[12], Étienne Artigau[7], Amanda Rose Arvai[3], Paul Atcheson[2,87], Charles B. Atkinson[14], Jesse Averbukh[3], Cagatay Aymergen[1], John J. Bacinski[3], Wayne E. Baggett[3], Giorgio Bagnasco[11], Lynn L. Baker[1], Vicki Ann Balzano[3], Kimberly A. Banks[1], David A. Baran[1], Elizabeth A. Barker[3], Larry K. Barrett[1], Bruce O. Barringer[3], Allison Barto[2], William Bast[3], Pierre Baudoz[16], Stefi Baum[17], Thomas G. Beatty[18], Mathilde Beaulieu[19], Kathryn Bechtold[3], Tracy Beck[3], Megan M. Beddard[3], Charles Beichman[20], Larry Bellagama[14], Pierre Bely[3,87], Timothy W. Berger[14], Louis E. Bergeron[3], Antoine-Darveau Bernier[7], Maria D. Bertch[3], Charlotte Beskow[6], Laura E. Betz[1], Carl P. Biagetti[3], Stephan Birkmann[21], Kurt F. Bjorklund[14], James D. Blackwood[1], Ronald Paul Blazek[3], Stephen Blossfeld[14], Marcel Bluth[22], Anthony Boccaletti[16], Martin E. Boegner Jr[3], Ralph C. Bohlin[3], John Joseph Boia[3], Torsten Böker[21], N. Bonaventura[23], Nicholas A. Bond[1,24], Kari Ann Bosley[3], Rene A. Boucarut[1], Patrice Bouchet[25], Jeroen Bouwman[26], Gary Bower[3], Ariel S. Bowers[3], Charles W. Bowers[1], Leslye A. Boyce[1], Christine T. Boyer[3], Martha L. Boyer[3], Michael Boyer[3], Robert Boyer[3], Larry D. Bradley[3], Gregory R. Brady[3], Bernhard R. Brandl[27], Judith L. Brannen[1], David Breda[28], Harold G. Bremmer[1,87], David Brennan[3], Pamela A. Bresnahan[3], Stacey N. Bright[3], Brian J. Broiles[1], Asa Bromenschenkel[3], Brian H. Brooks[3], Keira J. Brooks[3], Bob Brown[2,87], Bruce Brown[14], Thomas M. Brown[3], Barry W. Bruce[1,87], Jonathan G. Bryson[1], Edwin D. Bujanda[14], Blake M. Bullock[14], A. J. Bunker[29], Rafael Bureo[11], Irving J. Burt[1], James Aaron Bush[3], Howard A. Bushouse[3], Marie C. Bussman[1], Olivier Cabaud[6], Steven Cale[1], Charles D. Calhoon[1], Humberto Calvani[3], Alicia M. Canipe[3], Francis M. Caputo[3], Mihai Cara[3], Larkin Carey[2], Michael Eli Case[3], Thaddeus Cesari[1], Lee D. Cetorelli[1,87], Don R. Chance[3], Lynn Chandler[1], Dave Chaney[2], George N. Chapman[3], S. Charlot[30], Pierre Chayer[3], Jeffrey I. Cheezum[14], Bin Chen[3], Christine H. Chen[3], Brian Cherinka[3], Sarah C. Chichester[3], Zachary S. Chilton[3], Dharini Chittiraibalan[3], Mark Clampin[31], Charles R. Clark[1], Kerry W. Clark[3], Stephanie M. Clark[1], Edward E. Claybrooks[1], Keith A. Cleveland[1], Andrew L. Cohen[14], Lester M. Cohen[32], Knicole D. Colón[1], Benee L. Coleman[3], Luis Colina[12], Brian J. Comber[1], Thomas M. Comeau[3], Thomas Comer[3], Alain Conde Reis[6], Dennis C. Connolly[1], Kyle E. Conroy[3], Adam R. Contos[2,33], James Contreras[2], Neil J. Cook[7], James L. Cooper[1], Rachel Aviva Cooper[3], Michael F. Correia[1], Matteo Correnti[3], Christophe Cossou[34], Brian F. Costanza[14], Alain Coulais[35], Colin R. Cox[3], Ray T. Coyle[14], Misty M. Cracraft[3], Keith A. Crew[3], Gary J. Curtis[3], Bianca Cusveller[11], Cleyciane Da Costa Maciel[36], Christopher T. Dailey[1], Frédéric Daugeron[6], Greg S. Davidson[14], James E. Davies[3], Katherine Anne Davis[3], Michael S. Davis[1], Ratna Day[1], Daniel de Chambure[6,36], Pauline de Jong[36,11], Guido De Marchi[11], Bruce H. Dean[1], John E. Decker[1,87], Amy S. Delisa[1], Lawrence C. Dell[1], Gail Dellagatta[1,87], Franciszka Dembinska[6], Sandor Demosthenes[2], Nadezhda M. Dencheva[3], Philippe Deneu[37], William W. DePriest[3], Jeremy Deschenes[3], Nathalie Dethienne[37], Örs Hunor Detre[26], Rosa Izela Diaz[3], Daniel Dicken[38], Audrey S. DiFelice[3], Matthew Dillman[3], Maureen O. Disharoon[1], William V. Dixon[3], Jesse B. Doggett[3], Keisha L. Dominguez[1], Thomas S. Donaldson[3], Cristina M. Doria-Warner[1], Tony Dos Santos[36], Heather Doty[2], Robert E. Douglas, Jr[3], René Doyon[7], Alan Dressler[39], Jennifer Driggers[1], Phillip A. Driggers[1], Jamie L. Dunn[1], Kimberly C. DuPrie[3], Jean Dupuis[40], John Durning[1,87], Sanghamitra B. Dutta[31], Nicholas M. Earl[3], Paul Eccleston[41], Pascal Ecobichon[37], Eiichi Egami[8], Ralf Ehrenwinkler[10], Jonathan D. Eisenhamer[3], Michael Eisenhower[32], Daniel J. Eisenstein[32], Zaky El Hamel[11], Michelle L. Elie[3], James Elliott[3], Kyle Wesley Elliott[3], Michael Engesser[3], Néstor Espinoza[3], Odessa Etienne[3], Mireya Etxaluze[41], Leah Evans[3], Luce Fabreguettes[6], Massimo Falcolini[11], Patrick R. Falini[3], Curtis Fatig[1,87], Matthew Feeney[3], Lee D. Feinberg[1], Raymond Fels[11], Nazma Ferdous[3], Henry C. Ferguson[3], Laura Ferrarese[42], Marie-Héléne Ferreira[36], Pierre Ferruit[11,13], Malcolm Ferry[43], Joseph Charles Filippazzo[3], Daniel Firre[44], Mees Fix[3], Nicolas Flagey[3], Kathryn A. Flanagan[3], Scott W. Fleming[3], Michael Florian[8], James R. Flynn[14], Luca Foiadelli[44], Mark R. Fontaine[1,87], Erin Marie Fontanella[3], Peter Randolph Forshay[3], Elizabeth A. Fortner[1,87], Ori D. Fox[3], Alexandro P. Framarini[3], John I. Francisco[14], Randy Franck[2], Marijn Franx[27], David E. Franz[1], Scott D. Friedman[3], Katheryn E. Friend[14], James R. Frost[1], Henry Fu[14], Alexander W. Fullerton[3], Lionel Gaillard[11], Sergey Galkin[3], Ben Gallagher[2,45], Anthony D. Galyer[1], Macarena García Marín[21], Lisa E. Gardner[3], Dennis Garland[3], Bruce Albert Garrett[3], Danny Gasman[15], András Gáspár[8], René Gastaud[25], Daniel Gaudreau[40], Peter Timothy Gauthier[3], Vincent Geers[38], Paul H. Geithner[1], Mario Gennaro[3], John Gerber[2,87], John C. Gereau[14], Robert Giampaoli[14], Giovanna Giardino[21], Paul C. Gibbons[1], Karoline Gilbert[3], Larry Gilman[14], Julien H. Girard[3], Mark E. Giuliano[3], Konstantinos Gkountis[6], Alistair Glasse[38], Kirk Zachary Glassmire[3], Adrian Michael Glauser[46], Stuart D. Glazer[1], Joshua Goldberg[3], David A. Golimowski[3], Shireen P. Gonzaga[3],

Karl D. Gordon[3], Shawn J. Gordon[14], Paul Goudfrooij[3], Michael J. Gough[3], Adrian J. Graham[11], Christopher M. Grau[1], Joel David Green[3], Gretchen R. Greene[3], Thomas P. Greene[47], Perry E. Greenfield[3], Matthew A. Greenhouse[1], Thomas R. Greve[48], Edgar M. Greville[1], Stefano Grimaldi[2], Frank E. Groe[14], Andrew Groebner[3], David M. Grumm[3], Timothy Grundy[41], Manuel Güdel[49], Pierre Guillard[30], John Guldalian[14], Christopher A. Gunn[1], Anthony Gurule[2], Irvin Meyer Gutman[3], Paul D. Guy[1,88], Benjamin Guyot[6], Warren J. Hack[3], Peter Haderlein[28], James B. Hagan[3], Andria Hagedorn[14], Kevin Hainline[8], Craig Haley[9], Maryam Hami[3], Forrest Clifford Hamilton[3], Jeffrey Hammann[14], Heidi B. Hammel[50], Christopher J. Hanley[3], Carl August Hansen[3], Bruce Hardy[2,87], Bernd Harnisch[11,87], Michael Hunter Harr[3], Pamela Harris[1], Jessica Ann Hart[3], George F. Hartig[3], Hashima Hasan[31], Kathleen Marie Hashim[3], Ryan Hashimoto[14], Sujee J. Haskins[1], Robert Edward Hawkins[3,88], Brian Hayden[3], William L. Hayden[1,87], Mike Healy[11], Karen Hecht[3], Vince J. Heeg[14], Reem Hejal[14], Kristopher A. Helm[14], Nicholas J. Hengemihle[1], Thomas Henning[26], Alaina Henry[3], Ronald L. Henry[3], Katherine Henshaw[3], Scarlin Hernandez[3], Donald C. Herrington[3], Astrid Heske[11], Brigette Emily Hesman[3], David L. Hickey[3], Bryan N. Hilbert[3], Dean C. Hines[3], Michael R. Hinz[14], Michael Hirsch[14], Robert S. Hitcho[3], Klaus Hodapp[51], Philip E. Hodge[3], Melissa Hoffman[3], Sherie T. Holfeltz[3], Bryan Jason Holler[3], Jennifer Rose Hoppa[3], Scott Horner[47], Joseph M. Howard[1], Richard J. Howard[31,87], Jean M. Huber[1], Joseph S. Hunkeler[3], Alexander Hunter[3], David Gavin Hunter[3], Spencer W. Hurd[1], Brendan J. Hurst[3], John B. Hutchings[42], Jason E. Hylan[1], Luminita Ilinca Ignat[40], Garth Illingworth[52], Sandra M. Irish[1], John C. Isaacs III[3], Wallace C. Jackson Jr[14], Daniel T. Jaffe[53], Jasmin Jahic[14], Amir Jahromi[1], Peter Jakobsen[23], Bryan James[1], John C. James[1], LeAndrea Rae James[3], William Brian Jamieson[3], Raymond D. Jandra[14], Ray Jayawardhana[54], Robert Jedrzejewski[3], Basil S. Jeffers[1], Peter Jensen[11], Egges Joanne[2,87], Alan T. Johns[1], Carl A. Johnson[3], Eric L. Johnson[1], Patricia Johnson[1,87], Phillip Stephen Johnson[3], Thomas K. Johnson[1], Timothy W. Johnson[3], Doug Johnstone[42,55], Delphine Jollet[11], Danny P. Jones[3], Gregory S. Jones[14], Olivia C. Jones[38], Ronald A. Jones[1], Vicki Jones[3], Ian J. Jordan[3], Margaret E. Jordan[3], Reginald Jue[14], Mark H. Jurkowski[1], Grant Justis[3], Kay Justtanont[56], Catherine C. Kaleida[3], Jason S. Kalirai[57], Phillip Cabrales Kalmanson[3], Lisa Kaltenegger[54], Jens Kammerer[3], Samuel K. Kan[14], Graham Childs Kanarek[3], Shaw-Hong Kao[3], Diane M. Karakla[3], Hermann Karl[10], Susan A. Kassin[3,58], David D. Kauffman[3], Patrick Kavanagh[59], Leigh L. Kelley[1], Douglas M. Kelly[8], Sarah Kendrew[21], Herbert V. Kennedy[3], Deborah A. Kenny[3], Ritva A. Keski-Kuha[1], Charles D. Keyes[3], Ali Khan[11], Richard C. Kidwell[3], Randy A. Kimble[1], James S. King[1,87], Richard C. King[1], Wayne M. Kinzel[3], Jeffrey R. Kirk[1], Marc E. Kirkpatrick[14], Pamela Klaassen[38], Lana Klingemann[2], Paul U. Klintworth[14], Bryan Adam Knapp[3], Scott Knight[2], Perry J. Knollenberg[14], Daniel Mark Knutsen[3], Robert Koehler[3], Anton M. Koekemoer[3], Earl T. Kofler[14], Vicki L. Kontson[1], Aiden Rose Kovacs[3], Vera Kozhurina-Platais[3], Oliver Krause[26], Gerard A. Kriss[3], John Krist[28], Monica R. Kristoffersen[14], Claudia Krogel[1], Anthony P. Krueger[3], Bernard A. Kulp[3], Nimisha Kumari[21], Sandy W. Kwan[28], Mark Kyprianou[3], Aurora Gadiano Labador[3], Álvaro Labiano[60], David Lafrenière[7], Pierre-Olivier Lagage[34], Victoria G. Laidler[3], Benoit Laine[11], Simon Laird[11], Charles-Philippe Lajoie[3], Matthew D. Lallo[3], May Yen Lam[3], Stephanie Marie LaMassa[3], Scott D. Lambros[1], Richard Joseph Lampenfield[3], Matthew Ed Lander[1], James Hutton Langston[3], Kirsten Larson[21], Melora Larson[28], Robert Joseph LaVerghetta[3], David R. Law[3], Jon F. Lawrence[1], David W. Lee[14], Janice Lee[3,8,61], Yat-Ning Paul Lee[3], Jarron Leisenring[8], Michael Dunlap Leveille[3], Nancy A. Levenson[3], Joshua S. Levi[14], Marie B. Levine[28], Dan Lewis[43], Jake Lewis[2,62], Nikole Lewis[54], Mattia Libralato[21], Norbert Lidon[37], Paula Louisa Liebrecht[3], Paul Lightsey[2,87], Simon Lilly[46], Frederick C. Lim[1], Pey Lian Lim[3], Sai-Kwong Ling[14], Lisa J. Link[1], Miranda Nicole Link[3], Jamie L. Lipinski[3], XiaoLi Liu[3], Amy S. Lo[14], Lynette Lobmeyer[2], Ryan M. Logue[3], Chris A. Long[3], Douglas R. Long[3], Ilana D. Long[3], Knox S. Long[3], Marcos López-Caniego[63], Jennifer M. Lotz[3], Jennifer M. Love-Pruitt[14], Michael Lubskiy[3], Edward B. Luers[1,87], Robert A. Luetgens[14], Annetta J. Luevano[14], Sarah Marie G. Flores Lui[3], James M. Lund III[14], Ray A. Lundquist[31], Jonathan Lunine[54], Nora Lützgendorf[21], Richard J. Lynch[1,64], Alex J. MacDonald[3], Kenneth MacDonald[3], Matthew J. Macias[14], Keith I. Macklis[14], Peiman Maghami[1], Rishabh Y. Maharaja[1], Roberto Maiolino[65,66], Konstantinos G. Makrygiannis[14], Sunita Giri Malla[3], Eliot M. Malumuth[1], Elena Manjavacas[21], Andrea Marini[11], Amanda Marrione[3], Anthony Marston[13], André R Martel[3], Didier Martin[11], Peter G. Martin[67], Kristin L. Martinez[2], Marc Maschmann[10], Gregory L. Masci[3], Margaret E. Masetti[1,24], Michael Maszkiewicz[40], Gary Matthews[1], Jacob E. Matuskey[3], Glen A. McBrayer[14], Donald W. McCarthy[8], Mark J. McCaughrean[11], Leslie A. McClare[1], Michael D. McClare[1], John C. McCloskey[1], Taylore D. McClurg[14], Martin McCoy[1], Michael W. McElwain[1], Roy D. McGregor[14], Douglas B. McGuffey[1], Andrew G. McKay[14], William K. McKenzie[1], Brian McLean[3], Matthew McMaster[3], Warren McNeil[1,87], Wim De Meester[15], Kimberly L. Mehalick[1], Margaret Meixner[3], Marcio Meléndez[3], Michael P. Menzel[1], Michael T. Menzel[1], Matthew Merz[3], David D. Mesterharm[1], Michael R. Meyer[68], Michele L. Meyett[3], Luis E. Meza[14], Calvin Midwinter[9], Stefanie N. Milam[1], Jay Todd Miller[3], William C. Miller[1], Cherie L. Miskey[1], Karl Misselt[8], Eileen P. Mitchell[1], Martin Mohan[14], Emily E. Montoya[1], Michael J. Moran[14], Takahiro Morishita[3], Amaya Moro-Martín[3], Debra L. Morrison[3], Jane Morrison[8], Ernie C. Morse[3], Michael Moschos[14], S. H. Moseley[1,69], Gary E. Mosier[1], Peter Mosner[10], Matt Mountain[50], Jason S. Muckenthaler[14], Donald G. Mueller[3], Migo Mueller[70], Daniella Muhiem[1,88], Prisca Mühlmann[11], Susan Elizabeth Mullally[3], Stephanie M. Mullen[1], Alan J Munger[14], Jess Murphy[2], Katherine T. Murray[3], James C. Muzerolle[3], Matthew Mycroft[28], Andrew Myers[3], Carey R. Myers[3], Fred Richard R. Myers[14], Richard Myers[14], Kaila Myrick[3], Adrian F. Nagle, IV[2], Omnarayani Nayak[3], Bret Naylor[28], Susan G. Neff[1], Edmund P. Nelan[3], John Nella[14],

Duy Tuong Nguyen[3], Michael N. Nguyen[1], Bryony Nickson[3], John Joseph Nidhiry[3], Malcolm B. Niedner[1,87], Maria Nieto-Santisteban[3], Nikolay K. Nikolov[3], Mary Ann Nishisaka[14], Alberto Noriega-Crespo[3], Antonella Nota[21,87], Robyn C. O'Mara[1], Michael Oboryshko[3], Marcus B. O'Brien[14], William R. Ochs[1,87], Joel D. Offenberg[71,72], Patrick Michael Ogle[3], Raymond G. Ohl[1], Joseph Hamden Olmsted[3], Shannon Barbara Osborne[3], Brian Patrick O'Shaughnessy[3], Göran Östlin[73], Brian O'Sullivan[21], O. Justin Otor[3], Richard Ottens[1], Nathalie N.-Q. Ouellette[7], Daria J. Outlaw[1], Beverly A. Owens[3], Camilla Pacifici[3], James Christophe Page[3], James G. Paranilam[3], Sang Park[32], Keith A. Parrish[1], Laura Paschal[1], Polychronis Patapis[46], Jignasha Patel[1], Keith Patrick[14], Robert A. Pattishall Jr[14], Douglas William Paul[3], Shirley J. Paul[1], Tyler Andrew Pauly[3], Cheryl M. Pavlovsky[3], Maria Peña-Guerrero[3], Andrew H. Pedder[3], Matthew Weldon Peek[3], Patricia A. Pelham[3], Konstantin Penanen[28], Beth A. Perriello[3], Marshall D. Perrin[3], Richard F. Perrine[3], Chuck Perrygo[1,87], Muriel Peslier[36], Michael Petach[14], Karla A. Peterson[3], Tom Pfarr[1,87], James M. Pierson[1], Martin Pietraszkiewicz[14], Guy Pilchen[6], Judy L. Pipher[74], Norbert Pirzkal[21], Joseph T. Pitman[1], Danielle M. Player[3], Rachel Plesha[3], Anja Plitzke[11], John A. Pohner[14], Karyn Konstantin Poletis[3], Joseph A. Pollizzi[3], Ethan Polster[3], James T. Pontius[1], Klaus Pontoppidan[3], Susana C. Porges[14], Gregg D. Potter[14], Stephen Prescott[3], Charles R. Proffitt[3], Laurent Pueyo[3], Irma Aracely Quispe Neira[3], Armando Radich[1,87], Reiko T. Rager[3], Julien Rameau[7,75], Deborah D. Ramey[1,88], Rafael Ramos Alarcon[3], Riccardo Rampini[11], Robert Rapp[1], Robert A. Rashford[1], Bernard J. Rauscher[1], Swara Ravindranath[3], Timothy Rawle[21], Tynika N. Rawlings[1], Tom Ray[59], Michael W. Regan[3], Brian Rehm[1,87], Kenneth D. Rehm[76], Neill Reid[3], Carl A. Reis[1], Florian Renk[44], Tom B. Reoch[14], Michael Ressler[28], Armin W. Rest[3], Paul J. Reynolds[14], Joel G. Richon[3], Karen V. Richon[1], Michael Ridgaway[3], Adric Richard Riedel[3], George H. Rieke[8], Marcia J. Rieke[8], Richard E. Rifelli[14], Jane R. Rigby[1], Catherine S. Riggs[3], Nancy J. Ringel[1], Christine E. Ritchie[3], Hans-Walter Rix[26], Massimo Robberto[3,58], Gregory L. Robinson[31,87], Michael S. Robinson[3], Orion Robinson[3], Frank W. Rock[3], David R. Rodriguez[3], Bruno Rodríguez del Pino[12], Thomas Roellig[47], Scott O. Rohrbach[1], Anthony J. Roman[3], Frederick J. Romelfanger[3], Felipe P. Romo Jr[1], Jose J. Rosales[1], Perry Rose[3], Anthony F. Roteliuk[14], Marc N. Roth[14], Braden Quinn Rothwell[3], Sylvain Rouzaud[37], Jason Rowe[77], Neil Rowlands[9], Arpita Roy[3], Pierre Royer[15], Chunlei Rui[14], Peter Rumler[11,87], William Rumpl[3], Melissa L. Russ[3], Michael B. Ryan[14], Richard M. Ryan[31], Karl Saad[40], Modhumita Sabata[3], Rick Sabatino[1], Elena Sabbi[3], Phillip A. Sabelhaus[1,88], Stephen Sabia[1], Kailash C. Sahu[3], Babak N. Saif[1,3], Jean-Christophe Salvignol[11], Piyal Samara-Ratna[78], Bridget S. Samuelson[14], Felicia A. Sanders[28], Bradley Sappington[3], B. A. Sargent[3,58], Arne Sauer[10], Bruce J. Savadkin[1,87], Marcin Sawicki[79], Tina M. Schappell[1], Caroline Scheffer[11], Silvia Scheithauer[26], Ron Scherer[14], Conrad Schiff[1], Everett Schlawin[8], Olivier Schmeitzky[11], Tyler S. Schmitz[3], Donald J. Schmude[14], Analyn Schneider[28], Jürgen Schreiber[26], Hilde Schroeven-Deceuninck[11], John J. Schultz[3], Ryan Schwab[3], Curtis H. Schwartz[1], Dario Scoccimarro[6], John F. Scott[3], Michelle B. Scott[1], Bonita L. Seaton[1], Bruce S. Seely[3], Bernard Seery[80], Mark Seidleck[1,87], Kenneth Sembach[3], Clare Elizabeth Shanahan[3], Bryan Shaughnessy[41], Richard A. Shaw[3], Christopher Michael Shay[3], Even Sheehan[1], Kartik Sheth[31], Hsin-Yi Shih[3], Irene Shivaei[8], Noah Siegel[2], Matthew G. Sienkiewicz[3], Debra D. Simmons[14], Bernard P. Simon[3], Marco Sirianni[21], Anand Sivaramakrishnan[3,58,81], Jeffrey E. Slade[1], G. C. Sloan[3], Christine E. Slocum[3], Steven E. Slowinski[3], Corbett T. Smith[1], Eric P. Smith[31], Erin C. Smith[1], Koby Smith[2], Robert Smith[82], Stephanie J. Smith[3], John L. Smolik[14], David R. Soderblom[3], Sangmo Tony Sohn[3], Jeff Sokol[2], George Sonneborn[1,87], Christopher D. Sontag[3], Peter R. Sooy[1], Remi Soummer[3], Dana M. Southwood[14], Kay Spain[3], Joseph Sparmo[1], David T. Speer[1], Richard Spencer[3], Joseph D. Sprofera[14], Scott S. Stallcup[3], Marcia K. Stanley[1], John A. Stansberry[3], Christopher C. Stark[1], Carl W. Starr[1], Diane Y. Stassi[1], Jane A. Steck[1], Christine D. Steeley[1], Matthew A. Stephens[1], Ralph J. Stephenson[14], Alphonso C. Stewart[1], Massimo Stiavelli[3], Hervey Stockman Jr[3,87], Paolo Strada[11], Amber N. Straughn[1], Scott Streetman[2], David Kendal Strickland[3], Jingping F. Strobele[14], Martin Stuhlinger[13], Jeffrey Edward Stys[3], Miguel Such[11], Kalyani Sukhatme[28], Joseph F. Sullivan[2,87], Pamela C. Sullivan[1], Sandra M. Sumner[1], Fengwu Sun[8], Benjamin Dale Sunnquist[3], Daryl Allen Swade[3], Michael S. Swam[3], Diane F. Swenton[1], Robby A. Swoish[14], Oi In Tam Litten[3], Laszlo Tamas[38], Andrew Tao[14], David K. Taylor[3], Joanna M. Taylor[3], Maurice te Plate[21], Mason Van Tea[3], Kelly K. Teague[3], Randal C. Telfer[3], Tea Temim[83], Scott C. Texter[14], Deepashri G. Thatte[3], Christopher Lee Thompson[3], Linda M. Thompson[3], Shaun R. Thomson[1], Harley Thronson[1,87], C. M. Tierney[14], Tuomo Tikkanen[78], Lee Tinnin[8], William Thomas Tippet[3], Connor William Todd[3], Hien D. Tran[3], John Trauger[28], Edwin Gregorio Trejo[3], Justin Hoang Vinh Truong[3], Christine L. Tsukamoto[14], Yasir Tufail[3], Jason Tumlinson[3], Samuel Tustain[41], Harrison Tyra[3], Leonardo Ubeda[3], Kelli Underwood[3], Michael A. Uzzo[3], Steven Vaclavik[3], Frida Valenduc[36], Jeff A. Valenti[3], Julie Van Campen[1], Inge van de Wetering[11], Roeland P. Van Der Marel[3], Remy van Haarlem[11], Bart Vandenbussche[15], Ewine F. van Dishoeck[27], Dona D. Vanterpool[1], Michael R. Vernoy[14], Maria Begoña Vila Costas[1,22], Kevin Volk[3], Piet Voorzaat[11], Mark F. Voyton[1], Ekaterina Vydra[3], Darryl J. Waddy[1], Christoffel Waelkens[15], Glenn Michael Wahlgren[3], Frederick E. Walker Jr[14], Michel Wander[40], Christine K. Warfield[3], Gerald Warner[9], Francis C. Wasiak[1], Matthew F. Wasiak[1], James Wehner[14], Kevin R. Weiler[14], Mark Weilert[28], Stanley B. Weiss[14], Martyn Wells[38], Alan D. Welty[3], Lauren Wheate[1], Thomas P. Wheeler[3], Christy L. White[14], Paul Whitehouse[1], Jennifer Margaret Whiteleather[3], William Russell Whitman[3], Christina C. Williams[84], Christopher N. A. Willmer[8], Chris J. Willott[42], Scott P. Willoughby[14], Andrew Wilson[9], Debra Wilson[8], Donna V. Wilson[1], Rogier Windhorst[85], Emily Christine Wislowski[3], David J. Wolfe[3], Michael A. Wolfe[3], Schuyler Wolff[8], Amancio Wondel[36], Cindy Woo[14], Robert T. Woods[14], Elaine Worden[2,87], William Workman[3],

Gillian S. Wright[38], Carl Wu[1], Chi-Rai Wu[3], Dakin D. Wun[14], Kristen B. Wymer[3], Thomas Yadetie[3], Isabelle C. Yan[1], Keith C. Yang[14], Kayla L. Yates[3], Christopher R. Yeager[3], Ethan John Yerger[3], Erick T. Young[80], Gary Young[14], Gene Yu[14], Susan Yu[3], Dean S. Zak[3], Peter Zeidler[86], Robert Zepp[3], Julia Zhou[9], Christian A. Zincke[1], Stephanie Zonak[3], and Elisabeth Zondag[11]

[1] NASA Goddard Space Flight Center, 8800 Greenbelt Road, Greenbelt, MD 20771, USA; jonathan.p.gardner@nasa.gov
[2] Ball Aerospace & Technologies Corp., 1600 Commerce Street, Boulder, CO 80301, USA
[3] Space Telescope Science Institute, 3700 San Martin Drive, Baltimore, MD, 21218, USA
[4] Department of Astronomy & Astrophysics, University of Toronto, 50 Saint George Street, Toronto, ON M5S 3H4, Canada
[5] Dunlap Institute for Astronomy and Astrophysics, University of Toronto, 50 Saint George Street, Toronto, ON M5S 3H4, Canada
[6] European Space Agency, HQ Daumesnil, 52 rue Jacques Hillairet, F-75012 Paris, France
[7] Institut de Recherche sur les Exoplanètes (iREx), Université de Montréal, Département de Physique, C.P. 6128 Succursale Centre-ville, Montréal, QC H3C 3J7, Canada
[8] Steward Observatory, University of Arizona, 933 North Cherry Avenue, Tucson, AZ 85721, USA
[9] Honeywell Aerospace #100, 303 Terry Fox Drive, Ottawa, ON K2K 3J1, Canada
[10] Airbus Defence and Space GmbH, Ottobrunn, Germany
[11] European Space Agency, European Research & Technology Centre, Keplerlaan 1, Postbus 299, 2200 AG Noordwijk, The Netherlands
[12] Centro de Astrobiología (CAB, CSIC-INTA), Carretera de Ajalvir, E-28850 Torrejón de Ardoz, Madrid, Spain
[13] European Space Agency, European Space Astronomy Centre, Camino bajo del Castillo, s/n, Urbanización Villafranca del Castillo, E-28692 Villanueva de la Cañada, Madrid, Spain
[14] Northrop Grumman, One Space Park, Redondo Beach, CA 90278, USA
[15] Instituut voor Sterrenkunde, KU Leuven, Celestijnenlaan 200D, Bus-2410, B-3000 Leuven, Belgium
[16] LESIA, Observatoire de Paris, Université PSL, CNRS, Sorbonne Université, Université de Paris, 5 place Jules Janssen, F-92195 Meudon, France
[17] Faculty of Science, 230 Machray Hall, 186 Dysart Road, University of Manitoba, Winnipeg, MB R3T 2N2, Canada
[18] Department of Astronomy, University of Wisconsin-Madison, Madison, WI 53706, USA
[19] Université Côte d'Azur, Observatoire de la Côte d'Azur, CNRS, Laboratoire Lagrange, F-06108 Nice, France
[20] NASA Exoplanet Science Institute/IPAC, Jet Propulsion Laboratory, California Institute of Technology, 1200 East California Boulevard, Pasadena, CA 91125, USA
[21] European Space Agency, Space Telescope Science Institute, 3700 San Martin Drive, Baltimore, MD 21218, USA
[22] KBR, 7701 Greenbelt Road, Greenbelt, MD 20770, USA
[23] Cosmic Dawn Center (DAWN), Niels Bohr Institute, University of Copenhagen, Jagtvej 128, DK-2200, Denmark
[24] Adnet Systems, Inc., 6720B Rockledge Drive, Suite # 504, Bethesda, MD 20817, USA
[25] Laboratoire AIM Paris-Saclay, CEA-IRFU/SAp, CNRS, Université Paris Diderot, F-91191 Gif-sur-Yvette, France
[26] Max Planck Institute for Astronomy, Königstuhl 17, D-69117 Heidelberg, Germany
[27] Leiden Observatory, Leiden University, PO Box 9513, 2300 RA Leiden, The Netherlands
[28] Jet Propulsion Laboratory, California Institute of Technology, 4800 Oak Grove Drive, Pasadena, CA 91109, USA
[29] Department of Physics, University of Oxford, Denys Wilkinson Building, Keble Road, Oxford, OX1 3RH, UK
[30] Sorbonne Université, UPMC-CNRS, UMR7095, Institut d'Astrophysique de Paris, F-75014 Paris, France
[31] NASA Headquarters, 300 E Street SW, Washington, DC 20546, USA
[32] The Center for Astrophysics, 60 Garden Street, Cambridge, MA 02138, USA
[33] Moog Space and Defense Group, 5025 North Robb Street, Suite 500, Arvada, CO 80033, USA
[34] Université Paris-Saclay, Université de Paris, CEA, CNRS, AIM, F-91191 Gif-sur-Yvette, France
[35] LERMA (CNRS) & Observatoire de Paris, Paris, France
[36] European Space Agency, Centre Spatial Guyanais, BP816—Route Nationale 1, 97388 Kourou CEDEX, French Guiana, France
[37] Centre national d'études spatiales, Direction des Lanceurs, 52 rue Jacques Hillairet, F-75612 Paris CEDEX, France
[38] UK Astronomy Technology Centre, Royal Observatory Edinburgh, Blackford Hill, Edinburgh, EH9 3HJ, UK
[39] The Observatories, The Carnegie Institution for Science, 813 Santa Barbara Street, Pasadena, CA 91101, USA
[40] Canadian Space Agency, 6767 Route de l'Aéroport, Saint-Hubert, QC J3Y 8Y9, Canada
[41] RAL Space, STFC, Rutherford Appleton Laboratory, Harwell, Oxford, Didcot, OX11 0QX, UK
[42] NRC Herzberg, 5071 West Saanich Road, Victoria, BC V9E 2E7, Canada
[43] Lockheed Martin Advanced Technology Center, 3251 Hanover Street, Palo Alto, CA 94304, USA
[44] European Space Agency, European Space Operations Centre, Robert-Bosch-Strasse 5, D-64293 Darmstadt, Germany
[45] TMT International Observatory, 100 W. Walnut Street, Suite 300, Pasadena, CA, 91124, USA
[46] ETH Zurich, Wolfgang-Pauli-Str 27, CH-8093 Zurich, Switzerland
[47] NASA Ames Research Center, Space Science and Astrobiology Division, MS 245-6, Moffett Field, CA, 94035, USA
[48] DTU Space, Technical University of Denmark. Building 328, Elektrovej, DK-2800 Kgs. Lyngby, Denmark
[49] Dept. of Astrophysics, University of Vienna, Türkenschanzstr 17, A-1180 Vienna, Austria
[50] Associated Universities for Research in Astronomy, Inc., 1331 Pennsylvania Avenue Northwest, Suite 1475, Washington, DC 20004, USA
[51] Institute for Astronomy, 640 North Aohoku Place, Hilo, HI 96720, USA
[52] UCO/Lick Observatory, University of California, Santa Cruz, CA 95064, USA
[53] The University of Texas at Austin, Department of Astronomy RLM 16.342, Austin, TX 78712, USA
[54] Department of Astronomy, Cornell University, Ithaca, NY 14853, USA
[55] Department of Physics and Astronomy, University of Victoria, Victoria, BC, V8P 5C2, Canada
[56] Dept. of Space, Earth and Environment, Chalmers University of Technology, Onsala Space Observatory, SE-43992 Onsala, Sweden
[57] Johns Hopkins University Applied Physics Laboratory, 11100 Johns Hopkins Road, Laurel, MD 20723, USA
[58] Dept. of Physics & Astronomy, Johns Hopkins University, 3400 North Charles Street, Baltimore, MD, 21218, USA
[59] Dublin Institute for Advanced Studies, School of Cosmic Physics, 31 Fitzwilliam Place, Dublin 2, D02 XF86, Ireland
[60] Telespazio UK for the European Space Agency, ESAC, Camino Bajo del Castillo s/n, E-28692 Villanueva de la Cañada, Spain
[61] Gemini Observatory/NSF's NOIRLab, 950 North Cherry Avenue, Tucson, AZ, 85719, USA
[62] Blue Canyon Technologies, 5330 Airport Road, Boulder, CO, 80301, USA
[63] Aurora Technology for the European Space Agency, ESAC, Madrid, Spain
[64] HelioSpace Inc., 932 Parker Street, Suite 2, Berkeley, CA, 94710, USA
[65] Cavendish Laboratory, University of Cambridge, 19 J.J. Thomson Avenue, Cambridge, CB3 0HE, UK
[66] Kavli Institute for Cosmology, University of Cambridge, Madingley Road, Cambridge, CB3 0HA, UK
[67] Canadian Institute for Theoretical Astrophysics, University of Toronto, McLennan Physical Laboratories, 60 Saint George Street, Toronto, Ontario, M5S 3H8, Canada

[68] Astronomy Department, University of Michigan, Ann Arbor, MI 48109, USA
[69] Quantum Circuits, Inc., New Haven, Connecticut, USA
[70] Kapteyn Astronomical Institute, University of Groningen, P.O. Box 800, 9700 AV Groningen, The Netherlands
[71] Vantage Systems Inc, Greenbelt, MD 20706, USA
[72] Howard Community College, Columbia, MD 21044, USA
[73] Department of Astronomy, Oskar Klein Centre, Stockholm University, SE-106 91 Stockholm, Sweden
[74] Department of Physics and Astronomy, University of Rochester, Rochester, NY 14627, USA
[75] Univ. Grenoble Alpes, CNRS, IPAG, F-38000 Grenoble, France
[76] Katherine Johnson IV&V Facility, Goddard Space Flight Center, Code 180, Greenbelt, MD 20771, USA
[77] Department of Physics & Astronomy, Bishop's University, Sherbrooke, QC J1M 1Z7, Canada
[78] School of Physics & Astronomy, Space Research Centre, University of Leicester, Space Park Leicester, 92 Corporation Road, Leicester, LE4 5SP, UK
[79] Institute for Computational Astrophysics and Department of Astronomy & Physics, Saint Mary's University, 923 Robie Street, Halifax, NS B3H 3C3, Canada
[80] Universities Space Research Association, 425 3rd Street Southwest, Suite 950, Washington DC 20024, USA
[81] Astrophysics Department, American Museum of Natural History, 79th Street at Central Park West, New York, NY 10024, USA
[82] Department of History and Classics, University of Alberta, Edmonton, Alberta, Canada
[83] Princeton University, 4 Ivy Lane, Princeton, NJ 08544, USA
[84] National Optical-Infrared Research Laboratory, 950 North Cherry Avenue, Tucson, AZ 85719, USA
[85] School of Earth and Space Exploration, Arizona State University, Tempe, AZ 85287-1404, USA
[86] AURA for the European Space Agency (ESA), ESA Office, Space Telescope Science Institute, 3700 San Martin Drive, Baltimore, MD 21218, USA
Received 2023 February 10; accepted 2023 May 2; published 2023 June 26

Abstract

Twenty-six years ago a small committee report, building on earlier studies, expounded a compelling and poetic vision for the future of astronomy, calling for an infrared-optimized space telescope with an aperture of at least 4 m. With the support of their governments in the US, Europe, and Canada, 20,000 people realized that vision as the 6.5 m James Webb Space Telescope. A generation of astronomers will celebrate their accomplishments for the life of the mission, potentially as long as 20 yr, and beyond. This report and the scientific discoveries that follow are extended thank-you notes to the 20,000 team members. The telescope is working perfectly, with much better image quality than expected. In this and accompanying papers, we give a brief history, describe the observatory, outline its objectives and current observing program, and discuss the inventions and people who made it possible. We cite detailed reports on the design and the measured performance on orbit.

Unified Astronomy Thesaurus concepts: Space vehicle instruments (1548); Astronomical instrumentation (799); Infrared astronomy (786); Infrared observatories (791); Space observatories (1543); History of astronomy (1868)

Supporting material: color figures

1. Introduction

We summarize the history, concept, scientific program, and technical performance of the James Webb Space Telescope (JWST, Webb; Gardner et al. 2006). This paper points to and extracts key results from detailed papers in this special issue on the four instruments: Near-Infrared Camera (NIRCam; Rieke et al. 2023, this issue), Near-Infrared Spectrograph (NIRSpec; Böker et al. 2023, this issue), Near-Infrared Imager and Slitless Spectrograph (NIRISS; Doyon et al. 2023, this issue), and Mid-Infrared Instrument (MIRI; Wright et al. 2023, this issue); the telescope (McElwain et al. 2023, this issue); the observatory (Menzel et al. 2023, this issue); the scientific performance (Rigby et al. 2023a, this issue); and the brightness of the sky and stray light (Rigby et al. 2023b, this issue).

JWST was launched on 2021 December 25, and is a 6.5m diameter cold space telescope with cameras and spectrometers covering 0.6–28μm wavelengths (see Figure 1). Orbiting the Sun-Earth L2 point, JWST extends the discoveries and technologies of the 2.4 m warm Hubble Space Telescope (HST) and the 85 cm cold Spitzer Space Telescope. JWST enables observations of the distant early universe, potentially reaching beyond redshift $z \sim 15$, which is within $\lesssim$300 Myr of the big bang. JWST's infrared wavelength range penetrates dust clouds to observe obscured active galactic nuclei (AGN), and star and planet formation. It shows objects that are too cool to radiate visible light. It also includes the fundamental vibration-rotation bands of important molecules.

JWST was conceived from the beginning as an international project. It was led by NASA in partnership with the European and Canadian Space Agencies (ESA and CSA). Observing time allocations are open to all astronomers worldwide. JWST was launched from French Guiana on an ESA-provided Ariane 5 rocket. JWST cost NASA $8.8B to get to launch and will make observations for a projected fuel-limited lifetime that is potentially as long as 20 yr. JWST's observations cannot be obtained in any other way: Hubble has 1/6.25 of the collecting area, and as a room-temperature telescope, emits its own infrared beyond 1.7 μm. Spitzer was cold but had less than 2% of JWST's collecting area. For ground-based telescopes, the Earth's warm atmosphere results in a background that is 10^6–10^7 times higher and also blocks large regions of infrared wavelengths.

JWST includes a general-purpose instrument package in its Integrated Science Instrument Module (ISIM). NIRCam covers 0.6–5 μm with filters, a coronagraph, 0.″032 pixels in its short-wavelength channel, and a dichroic filter, which enables simultaneous observation in both the short- and long-wavelength bands. NIRSpec covers the same wavelength range with prisms and gratings, with fixed slits, an integral-field unit (IFU), and a microshutter array (MSA) to select up to 100

[87] Retired
[88] Deceased

Figure 1. JWST in the Northrop Grumman cleanroom following a sunshield deployment test.

(A color version of this figure is available in the online journal.)

simultaneous targets. NIRISS covers the same wavelength range with slitless spectroscopy and provides a non-redundant mask for coronagraphy. MIRI covers 5–28 μm with imaging, IFU spectroscopy, and coronagraphs. The Fine Guidance Sensor (FGS) senses pointing errors and feeds the attitude control system to maintain sharp images. ESA provided the NIRSpec with the detectors and microshutter array provided by Goddard, CSA provided the NIRISS and FGS, and a partnership of JPL and a European consortium provided MIRI. NIRCam, and the US portions of MIRI and NIRSpec were funded by NASA.

JWST's first year of observations includes nearly half of a year of guaranteed time observations that are allocated to the teams building the instruments, six interdisciplinary scientists, and the telescope scientist. There is also a set of 13 competitively selected Director's Discretionary Early Release Science (DD-ERS) programs with data that will immediately become public. The remaining observations were selected from over 1200 proposals through a dual-anonymous peer review, in which the identities of the proposers were not known to the reviewers. Anyone can propose, regardless of nationality or institution. There were 286 programs selected in Cycle 1, including 263 pointed programs, three pure-parallel programs, and 20 archival or theory programs. The Cycle 2 call received more than 1600 proposals, which were submitted by more than 5000 scientists from around the world. NASA provides funding for data analysis to US-based investigators who are awarded time on JWST, and for archival and theoretical research related to JWST.

JWST is a technical pioneer. It is the first deployable segmented space telescope, with mirror segments that are aligned and focused after launch. It has a remarkable cryogenic optical system that provides diffraction-limited images (Strehl ratio 0.8) at wavelengths that are as short as 1.1 μm. Its detectors are larger and more sensitive than previous generations. Its 6.0 K cryocooler for the mid-infrared instrument (MIRI) has no expendables and should last the duration of the mission. It uses cryogenic ASICs to control and read the near-infrared detectors. Its five-layer sunshield cools the telescope to between 35 and 55 K. Based on JWST's successes and its lessons learned, NASA is positioned to proceed to the 6 m near-infrared, optical, and UV flagship telescope that was recommended by the 2020 Decadal Survey (National Academies of Sciences & Medicine 2021), with the ability to directly detect Earth-like planets around Sun-like stars.

2. Timeline History of JWST

In this section, we present a brief timeline history of the concept, design, construction, and testing of JWST.

2.1. 1980s

In the 1980s, preliminary work by Garth Illingworth, Pierre Bély, Peter Stockman, and others on an 8–10 m passively cooled infrared telescope began at the Space Telescope Science Institute (STScI), following Riccardo Giacconi's advice to work on the "next big thing." Progress was reported at the STScI/NASA Next Generation Space Telescope (NGST) conference, 1989 September 13–15 (Bely et al. 1990). This international conference excited scientists and engineers with the scientific opportunities and technical challenges that are enabled by a very large cold infrared space telescope. A decade before that, in 1979, a National Academy of Sciences (NAS) report recommended the Shuttle Infrared Telescope Facility (SIRTF, later Spitzer; Field & Astronomy & Astrophysics Survey Committee 1983). This recommendation was made before the IRAS launch (1983 January 25). Goddard built the Cosmic Background Explorer (COBE) and launched it on 1989 November 18 to measure the Big Bang, the cosmic microwave background, and infrared background light. The release of the COBE results began the era of precision cosmology (Mather et al. 1994). The discovery of the primeval anisotropy led to the standard model of cosmology, in which gravity acting on density fluctuations could produce galaxies. To build the COBE, Goddard also developed expertise with cryogenic instrumentation and test programs, which would become essential for Webb.

2.2. 1990s

The Hubble was launched 1990 April 24 and its optical error was soon discovered. This led to two breakthroughs: learning to measure the optical error (spherical aberration) with phase diversity, and demonstrating the value of the planned servicing and repair of Hubble using the Space Shuttle in 1993. The development of the phase diversity algorithms was jointly done by STScI, Goddard, and JPL (Burrows et al. 1991; Fienup et al. 1993; Krist & Burrows 1995). The experience gained by the people working on the servicing missions, instrument upgrades, and spacecraft hardware repairs and replacements would be critically important for the development of the JWST because many of the younger engineers working on Hubble later became leaders of the Webb team. The Bahcall report (Decadal Survey: Bahcall & Astronomy & Astrophysics Survey Committee 1991) endorsed Spitzer (at that time called the Space Infrared Telescope Facility, SIRTF) and declared that the 1990s would be the "Decade of the Infrared." The AstroTech conference (Illingworth 1991) reviewed possibilities for large telescopes and cited the Bahcall report. In 1993, the Edison mission, a deployable 2m+ diameter infrared telescope, was proposed to ESA (Thronson et al. 1996). Larger format infrared detector arrays, in part spurred by the NICMOS development, enabled galaxy surveys (e.g., Gardner et al.

1993) and other near-infrared science with ground-based telescopes.

The Edison concept included passive cooling, and some of the people working on Edison brought that experience to the JWST team later. The Hubble phase retrieval algorithm was published and the Hubble optics were corrected in its first servicing mission. Soon after, NASA commissioned AURA's HST and Beyond committee, chaired by Alan Dressler, to write a report on potential successors to HST (Dressler & HST & Beyond Committee 1996). STScI sent a proposal entitled "High-Z" to NASA, suggesting that a telescope in a 1×3 au long elliptical orbit would be helpful to get outside the interference of the zodiacal dust cloud. In 1995, JPL submitted the MIRORS proposal to NASA for a passively cooled mid-infrared telescope (Wade et al. 1996).

2.2.1. 1995

On 1995 October 30, Ed Weiler of NASA HQ left a phone message for John Mather at Goddard, explaining that NASA was starting a study of what was then called the Next Generation Space Telescope (NGST) and inviting his participation. Within the context of the previous studies, and based on a draft of the HST and Beyond report, NGST would be a 4 m passively cooled infrared telescope making observations at $1\ \mu\mathrm{m} < \lambda < 5\ \mu\mathrm{m}$. GSFC chose Bernie Seery to manage the study. The Federal Government shut down 1995 November 14–19 and again 1995 December 16–1996 January 6. On 1996 January 6 to 8, a record blizzard closed the Washington DC area and nothing moved for a week. As a result, Mather did not attend the dramatic AAS meeting in San Antonio. This pivotal start foreshadowed Webb's future—its development was to be affected by more storms, government shutdowns, a terrorist attack, an earthquake in Virginia, a lightning strike, a hurricane in Texas, and the COVID pandemic, all of which would occur before Webb was launched.

On 1996 January 15, the Hubble Deep Field image was released at the AAS meeting, completely changing our view of galaxies in the universe (Williams et al. 1996). On 1996 January 17, Dan Goldin spoke to the AAS, saying, "Why do you ask for such a modest thing [4 m]? Why not go after six or seven meters?" He received a standing ovation, which turned out to be Webb's first (informal) peer review. Dressler also spoke to present the report at the meeting (Dressler & HST & Beyond Committee 1996). On 1996 January 22–25, Mather attended a conference in Johannesburg and met ESA counterparts for the first time to discuss ideas for the NGST. The final Dressler report appeared in 1996 May (Dressler & HST & Beyond Committee 1996). Wendy Freedman's Hubble Key Project reported on the Hubble Constant, discussing their initial values (around $60\,\mathrm{km\,s^{-1}\,Mpc^{-1}}$) and comparing them to others (up to $80\,\mathrm{km\,s^{-1}\,Mpc^{-1}}$) (Freedman et al. 2001, and references therein). Predictions of early galaxies that could be visible to Webb depend strongly on this number and would be important when a descope decision was taken in 2001.

2.2.2. 1996–1999

The year 1996 marked the industrial kickoff. Around May, GSFC presented NGST ideas to interested aerospace companies in a meeting that was held at the Space Telescope Science Institute (STScI). NASA issued a Cooperative Agreement Notice so the companies could compete for this new work. Two studies were chosen (TRW and Ball), and they and the Government/STScI teams reported in September. Jonathan Gardner, who was newly hired at Goddard, attended the meeting, learning about NGST for the first time. The reports said they could meet Goldin's cost target of \$0.5B, though what exactly was included in these estimates is unclear now. Outside this group, hardly anyone believed that such a low cost was possible.

In 1997, NASA solicited proposals for the Ad Hoc Science Working Group to advise NASA on the choice of scientific objectives and instruments; the committee first met later that year. In 1997, AURA issued a report "Visiting a Time When Galaxies Were Young," detailing the concepts that had been developed in 1996 (Stockman 1997). In 1998, a conference in Liège, Belgium reported progress developing science drivers and technological challenges (Kaldeich-Schürmann 1998) after ESA had established an NGST Task Force. The STScI was officially made the NGST Science Operations Center in a ceremony with Senator Barbara Mikulski and Administrator Goldin. The cosmic acceleration (dark energy) was discovered (Riess et al. 1998; Schmidt et al. 1998; Perlmutter et al. 1999), which added to the growing sense that NGST was key to studies of the distant universe because a dark-energy-dominated universe has galaxies that form at a higher redshift than in a matter-dominated flat universe. The conference "Science with the NGST (Next Generation Space Telescope)" was held at GSFC (Smith & Koratkar 1998).

On July 7, NASA selected Lockheed Martin and TRW to conduct Phase A mission studies, which are preliminary analyses of the design and cost. Discussions began with international partners about their possible roles while ESA, CSA, and the Japanese Space Agency (JAXA) participated in the ASWG. In September, just as hurricane Floyd approached, the NGST Science and Technology Exposition was held in Hyannis, MA and the choices of possible near-infrared spectrometer designs were presented (Smith & Long 2000). Mather & Stockman (2000) reported the early history of NGST and listed the instrument studies that were then underway. The microelectromechanical system (MEMS) concept for a multi-object spectrometer was favored over a Fourier spectrometer because the Fourier multiplex advantage does not apply if most of the sky is empty and detector noise is not high (Gardner & Satyapal 2000). Moseley et al. (1999) described the micro-shutter array, which has significant advantages in size, contrast, and cryogenic operation over the micromirror arrays that were developed by Texas Instruments for digital light projection (MacKenty & Stiavelli 2000).

The ASWG's final report recommended that NGST include a NIRCam, NIRSpec with a MEMS-based multi-object spectrograph capability, and a MIRI doing both imaging and spectroscopy. They gave three options for a fourth instrument: a tunable filter, a visible-light camera, or an integral-field spectrograph (Stockman & Mather 2001). By this time, JAXA had decided not to participate in the mission, and the ASWG recommended that NASA partner with ESA and CSA.

2.3. 2000s

Ed Weiler signed the Formulation Authorization Document in 1999, which defined NGST as a NASA priority, but including a mid-infrared capability was a goal rather than a requirement. The 2000 Decadal Survey ranked NGST as the highest priority in large space missions (McKee et al. 2001).

This ranking was predicated on the inclusion of a mid-infrared instrument, which established it as a requirement for the mission. NASA chose an Interim Science Working Group (ISWG) to write the specifications for the instruments and advise about the telescope. NASA and ESA formed a joint Mid-Infrared Steering Committee, which developed a concept for a mid-infrared instrument to do both imaging and spectroscopy. The agencies negotiated a partnership in which ESA would provide the optical bench, and NASA would provide the detectors and cooling system.

In 2001, while preparing the statement of work for the solicitation of the main industrial contract, Goddard descoped the telescope from 50 to 25 m^2 in collecting area, or 8 to 6.5 m in diameter. The descope was to address a mismatch between the budget and the scope in the solicitation. In mid-2002, NASA chose TRW to build the observatory, reserving the ISIM to be built by Goddard. NASA renamed NGST for James E. Webb, who was the second administrator of NASA, from 1961 to 1968. Webb was responsible for getting astronauts to the Moon in 8 yr and for expanding NASA's science program, which built space telescopes, sent probes to Venus and Mars, and started missions to the outer planets (Lambright 1995).

In 2002, NASA selected a proposal led by Marcia Rieke of the University of Arizona to build the NIRCam. In the same proposal call, NASA selected several members of the flight Science Working Group (SWG; see Table 1), including six interdisciplinary scientists and the US members of the MIRI science team. NASA signed memoranda of understanding with ESA and CSA, which detailed the international partnership. ESA would provide the launch vehicle, the NIRSpec, and the optical bench for MIRI. CSA would provide the FGS, and install a tunable-filter imager (TFI) on the other side of the FGS optical bench. However, the development of a cryogenic etalon meeting the requirements for the TFI would prove to be challenging and ultimately was not successful. The SWG also includes NASA Project Scientists and representatives of the partner agencies.

As the project entered its detailed design phase, Phil Sabelhaus was selected as the project manager. In late 2003, the part of TRW selected to build JWST was acquired by Northrop Grumman. Northrop, in consultation with Goddard and the optics Product Integrity Team, selected beryllium for the mirror material. The competing glass sandwich technology had failed to meet its figure stability requirements (Stahl et al. 2004). In addition, the Spitzer Space Telescope (building on other infrared space missions) had demonstrated that construction of a high-precision beryllium mirror was possible. In 2003, Northrop began the fabrication of the flight mirrors through a sub-contract to Ball Aerospace.

Beginning the mirrors was a key step and reflected the expectation that they could be a critical path pacing item. The Spitzer Space Telescope was launched 2003 August 25. Spitzer rapidly demonstrated the power of mid-infrared space missions (e.g., Werner et al. 2004), and confirmed the wisdom of including the MIRI in JWST. On 2004 March 3, construction of the JWST officially began. In 2005, in order to conserve mass, a helium pulse-tube cryocooler to be built by Northrop Grumman was chosen to replace the planned solid hydrogen cooler for the MIRI. Gardner et al. (2006) published a special issue of the journal Space Science Reviews, detailing the JWST's science objectives and design. In 2005, Mike Griffin replaced Sean O'Keefe as NASA Administrator, and in 2007 Griffin approved the contribution of the European Ariane 5 rocket for JWST. The final servicing mission for HST was conducted in 2009, which freed the large cleanroom at Goddard for the integration of the JWST instruments into the ISIM, the integration of the Optical Telescope Element (OTE), and the assembly of the ISIM and the OTE.

2.4. 2010s

In 2010, CSA realized that they would not be able to deliver the tunable-filter imager on schedule, removed the etalon, and redesigned the camera as the NIRISS (Doyon et al. 2012). The near-infrared detectors were found to be degrading and it became clear that they would have to be replaced (Rauscher 2014; Rauscher et al. 2014). The spacecraft and sunshield were also behind schedule.

Budget troubles mounted, and Senator Mikulski asked for an independent review and a realistic budget estimate that would not grow every year. Congress was very skeptical of the planned 2014 launch date and the budget. The HgCdTe detectors were found to be degrading in storage, and a new version was ordered. NASA responded to the growing concerns around schedule and cost by setting up a Test Assessment Team for advice on the testing path forward. In response to Senator Mikulski's request for a full review of what was going wrong, the NASA Administrator set up the Independent Comprehensive Review Panel (ICRP). The ICRP report was hard hitting and direct, confirming the basic soundness of the mission and concurring with the recommendations of the JWST project management that additional budget and schedule were needed. The formal recommendations were all accepted by the Administrator. The ICRP emphasized the scientific value of JWST, but outlined the budgetary issues that had plagued the project and recommended that a thorough Joint Cost and Schedule assessment be done quickly. Project Manager Phil Sabelhaus was replaced by Bill Ochs. In 2011, that budget assessment was finished and indicated that it would take a total budget of $8B to complete JWST with a launch in 2018, 4 yr later than planned.

Frustration with JWST led to a proposed zero budget by the House Appropriation Sub-Committee on 2011 July 7. A grassroots public effort was undertaken to support Senator Mikulski's efforts to restore the budget. The public support was remarkable. The effort paid off and agreement was reached to restore JWST. Consequently, JWST's budget of $8.0B to launch was approved by Congress late in 2011, but with strong language capping the cost. In 2012, the MIRI and NIRISS/FGS instruments arrived at GSFC. Although a derecho storm cut off all three electrical power lines to GSFC in the middle of a cryo-vacuum test, there was no damage to the JWST hardware. In 2013, the NIRCam and NIRSpec arrived at GSFC, and the four instruments were assembled into the ISIM by 2014. Altogether, three cryo-vac tests were done on the instrument module (Kimble et al. 2016; Greenhouse 2016). It was assembled to the telescope, and given vibration and acoustic tests at GSFC. Challenges during the three cryo-vac tests included a major snowstorm, a lightning strike on the building, and a fire in the clean room, which prompted evacuation of the personnel. No people or flight hardware were harmed in these events, which took place between 2014 and 2016.

The 18 primary mirror segments, the secondary mirror, the tertiary mirror, and the fine-steering mirror are all made of

Table 1
The JWST Science Working Group

Name	Institution	Position
Santiago Arribas	CSIC	NIRSpec Science Representative *
Mark Clampin	NASA/HQ	Observatory Project Scientist *
René Doyon	Univ of Montreal	CSA Representative
Pierre Ferruit	ESA	ESA Representative
Kathryn Flanagan	STScI, retired	STScI Representative *
Marijn Franx	Leiden University	NIRSpec Science Representative *
Jonathan Gardner	NASA/GSFC	Deputy Senior Project Scientist
Matthew Greenhouse	NASA/GSFC	ISIM Project Scientist
Heidi Hammel	AURA	Interdisciplinary Scientist
John Hutchings	DAO, retired	CSA Representative *
Peter Jakobsen	ESA, retired	ESA Representative *
Jason Kalirai	JHU/APL	STScI Representative *
Randy Kimble	NASA/GSFC	Integration, Test, & Commissioning Project Scientist
Nikole Lewis	Cornell University	STScI Representative *
Simon Lilly	ETH Zurich	Interdisciplinary Scientist
Jonathan Lunine	Cornell University	Interdisciplinary Scientist
Roberto Maiolino	University of Cambridge	NIRSpec Science Representative
John Mather	NASA/GSFC	Senior Project Scientist
Mark McCaughrean	ESA	Interdisciplinary Scientist
Michael McElwain	NASA/GSFC	Observatory Project Scientist
Matt Mountain	AURA	Telescope Scientist
Malcolm Niedner	NASA, retired	Deputy Senior Project Scientist/Technical
George Rieke	University of Arizona	MIRI Science Lead
Marcia Rieke	University of Arizona	NIRCam Principal Investigator
Jane Rigby	NASA/GSFC	Operations Project Scientist
Hans-Walter Rix	Max Planck Institute	NIRSpec Science Representative *
George Sonneborn	NASA, retired	Operations Project Scientist *
Massimo Stiavelli	STScI	Interdisciplinary Scientist
H. Peter Stockman	STScI, retired	STScI Representative *
Jeff Valenti	STScI	STScI Representative
Chris Willott	CNRC	NIRISS Science Lead
Rogier Windhorst	Arizona State University	Interdisciplinary Scientist
Gillian Wright	UKATC	MIRI European Principal Investigator

Note. The JWST Science Working Group (SWG) consists of GTOs, NASA Project Scientists, and representatives from ESA, CSA, and STScI. (*) designates a former member who was replaced by someone else. The NIRSpec Science Representative position rotated through several members of the NIRSpec team. The SWG first met on 2002 August 19 and disbanded at the end of JWST Commissioning, 2022 July 12.

beryllium with a gold optical coating. Of the 18 primary mirror segments, there are six each of three optical prescriptions, to enable the six-fold symmetry of the primary mirror. Three spare mirrors, one of each optical prescription, were also prepared. In order to meet the 25 nm root-mean-squared surface figure requirement for each mirror segment, the mirrors were initially polished to a surface accuracy of about 100 nm, using an iterative process. The segments' surface figures were then measured at the cyrogenic operating temperature in the X-Ray and Cryogenic Facility (XRCF) at NASA's Marshall Space Flight Center. Using those cryogenic measurements, the segments were polished again so that they would meet the surface figure at their operating temperature. The secondary, tertiary, and FSM were treated in a similar manner. The mirrors were then coated, underwent environmental testing, and acceptance testing at the operating temperatures was conducted again in the XRCF. The individual mirrors were complete by early 2012 (Feinberg et al. 2012).

Figure 2. The JWST telescope and ISIM in preparation for the OTIS thermal vacuum test at the Johnson Space Center's historic Chamber A.
(A color version of this figure is available in the online journal.)

With the mirrors complete, the hexapod actuators were assembled onto each mirror. Assembly of the primary mirror segments onto the backplane took place at Goddard during late 2015 and early 2016. The integration of the ISIM onto the back of the primary mirror was complete by 2016 May 24, at which time the assembled Optical Telescope element and ISIM became known as OTIS. Vibration and acoustic testing took place over the following year.

On 2017 May 7, the OTIS was flown to NASA's Johnson Space Center on a C5C aircraft, and spent 6 months there, including a 100 day-long full scale cryo-vac test (see Figure 2), right through Hurricane Harvey and 1.3 m of rain (Kimble et al. 2018). On 2018 February 2, the OTIS arrived at Northrop Grumman in Redondo Beach for integration with the warm spacecraft and sunshield, which themselves were undergoing their element-level acoustic and vibration tests (Menzel et al. 2023, this issue). In 2017, delays in the spacecraft (e.g., propulsion system welding problems) and the sunshield development at Northrop began to indicate that a 2018 launch was not likely. By early 2018 it was clear that added time and

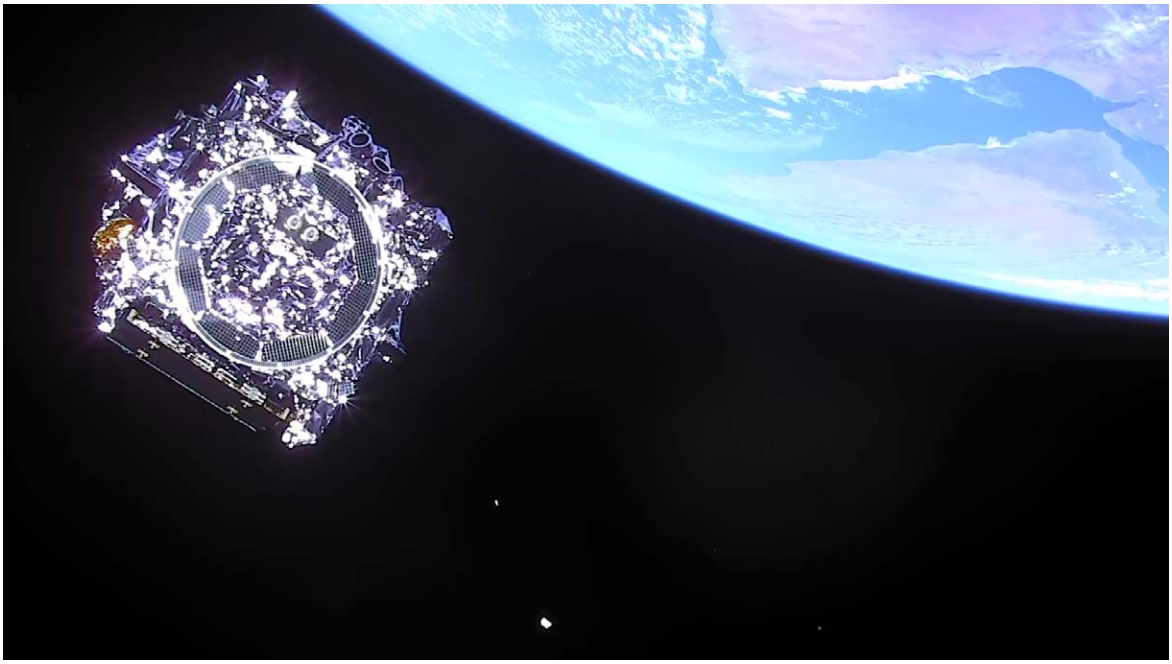

Figure 3. JWST viewed from a camera in the upper stage of the Ariane 5 launch vehicle, just after separation. The Gulf of Aden and the east coast of Africa are visible in the upper right. This still from a video is courtesy ESA and Arianespace. The full video is available at: https://www.esa.int/ESA_Multimedia/Videos/2021/12/Webb_separation_from_Ariane_5.

(A color version of this figure is available in the online journal.)

money was needed, and another Independent Review Team was set up. This team emphasized "mission success" but noted that a launch delay was inevitable for the integration and testing (I&T) that remained. In 2018 May, loose screws and washers were found after a vibration test of the sunshield, making it clear that a significant delay was necessary to get JWST back on track. Rework of the sunshield followed. A new launch date in 2020 was selected as likely.

During this decade, the Mission Operations Center was being set up at STScI and a major software development effort was being undertaken by STScI with GSFC management for mission operations, science support, and science operations. The JWST Science Advisory Committee (JSTAC) was chartered to help STScI and NASA develop science policies and approaches with the explicit goal of "maximizing the scientific return" from JWST. The JSTAC met for 8 yr in parallel to the SWG. Both advisory committees were eventually succeeded by the JWST Users Committee (JSTUC).

2.5. 2020s

Progress was good but the complexities of the I&T activities led to a further delay into 2021, which was compounded by the global coronavirus pandemic. In 2020 March, COVID-19 forced nationwide closures and NASA telework, but aerospace workers at the Northrop Grumman facility in California were permitted to work under enhanced COVID-19 safety procedures. After the final vibration and acoustic test in 2020, the flight transponders failed in early 2021 and were returned to the manufacturer for repair. Flight rehearsals began in the Mission Operations Center in 2020, using the digital twin—an observatory simulator that is still in use today for verification of command sequences. Some of the rehearsals included remote or hybrid participation due to the pandemic, which would prove valuable experience during commissioning.

The final I&T work in 2021 went extremely well, adding to confidence that the spacecraft and sunshield were becoming mature and ready for launch. On 2021 October 21, JWST arrived at the launch site in French Guiana on the MN Colibri ship, after passing through the Panama Canal. On 2021 December 25 at 12:20 UTC, the Ariane 5 launched the Webb exactly as planned, with a flawless launch and positioning of JWST for its trajectory to L2 (see Figure 3). The launch went so well that the propellant needed to adjust its trajectory to L2 and the insertion were much less than budgeted. The propellant available for orbit adjustment will likely allow a mission life extension to a predicted 20 yr, which is far larger than the 10 yr goal.

2.5.1. 2022

The first two weeks of "deployment terror" went remarkably well, with almost no unexpected issues. In particular, the sunshield with its 140 release mechanisms deployed successfully. The years of careful testing and checking had paid off. The following two weeks of mirror deployments also went smoothly and JWST was inserted into its L2 orbit 29 days after launch, ready for the slow and crucial process of aligning the mirrors. The outcome was that the optical performance and stability exceeded the requirements with 1.1 μm diffraction-limited imaging at NIRCam, or almost twice as good as the requirement (2 μm) (McElwain et al. 2023, this issue).

Despite the spike in COVID-19 cases at the end of 2021, the careful protocols that were developed and rehearsed by the Mission Operations Team enabled staffing of all critical ground-support positions throughout launch and early commissioning. Precautions included an expansion of the space used by the Mission Operations Center (MOC) at STScI to permit the staff to socially distance; greater reliance on remote support; mandated vaccination or testing, mandated masking,

and electronic contact tracing for personnel in the MOC; and rapid antigen testing every other day for on-site staff.

Overall, commissioning the observatory went extremely smoothly in the MOC, due to the prior tests and rehearsals, and especially the competence, focus and leadership throughout the NASA, Northrop, Ball, STScI, instrument teams, and other contractor teams. Everything on JWST works! Commissioning was completed and all 17 instrument modes were approved for scientific use by 2022 July 10. During commissioning, 120 hr were devoted to Early Release Observations (ERO; Pontoppidan et al. 2022). The ERO of SMACS 0723 was announced by President Biden at the White House July 11 (Figure 4), and Stephan's Quintet, the Carina Nebula, the Southern Ring Nebula, and WASP-96b were released on July 12. The data were released through the archives at the Mikulski Archive for Space Telescopes (MAST) on 2022 July 14; the release also included the commissioning data and online documentation of the scientific performance.

3. Science Scope

JWST was designed to address four science themes (Gardner et al. 2006), which trace cosmic history from the Big Bang to planets conducive to life. The End of the Dark Ages: First Light and Reionization theme seeks to identify the first luminous sources to form and to determine the ionization history of the early universe. The Assembly of Galaxies theme seeks to determine how galaxies and the dark matter, gas, stars, metals, morphological structures, and active nuclei within them evolved from the epoch of reionization to the present day. The Birth of Stars and Protoplanetary Systems theme seeks to unravel the birth and early evolution of stars, from infall on to dust-enshrouded protostars to the genesis of planetary systems. The Planetary Systems and the Origins of Life theme seeks to determine the physical and chemical properties of planetary systems, including our own, and investigate the potential for the origins of life in those systems.

Observing time on JWST has been allocated by three methods: Guaranteed Time Observations (GTO), General Observers (GO) time, and Director's Discretionary (DD) time. The GTO time consists of 4020 hr of JWST observations over the first three years, which are allocated to the four instrument teams and other scientists on the Science Working Group. The DD time consists of 10% of the time available for the lifetime of the mission. The GO time is the remainder.

The GTO allocations are listed in Table 2. Changes from the original allocations are due to programs shared between the GTOs and to changes in the overheads that occurred after the selected observations were specified prior to the Cycle 1 Call For Proposals. The GTO scientists chose to allocate the majority of the GTO time in Cycle 1, leaving just 196.1 hr of observation time for Cycles 2 and 3. This table shows the amount of time executed as of 2022 September 30. Further updates are available from https://www.stsci.edu/cgi-bin/get-jwst-gto-time.

The DD time is allocated by the Director of JWST's Science and Operations Center (SOC), located at the Space Telescope Science Institute. In 2018, following a recommendation by the JSTAC, Director Ken Sembach allocated up to 525 hr of Cycle 1 DD time to the DD-Early Release Science Program (Levenson & Sembach 2018). The DD-ERS program was designed and implemented by Janice Lee, Jennifer Lotz, and Neill Reid. It consists of 13 peer-review selected programs designed to demonstrate JWST's capabilities and provide open-access data to the community early in the mission. The DD-ERS programs were intended to be conducted within the first 3–5 months of Cycle 1; Table 3 lists the programs.

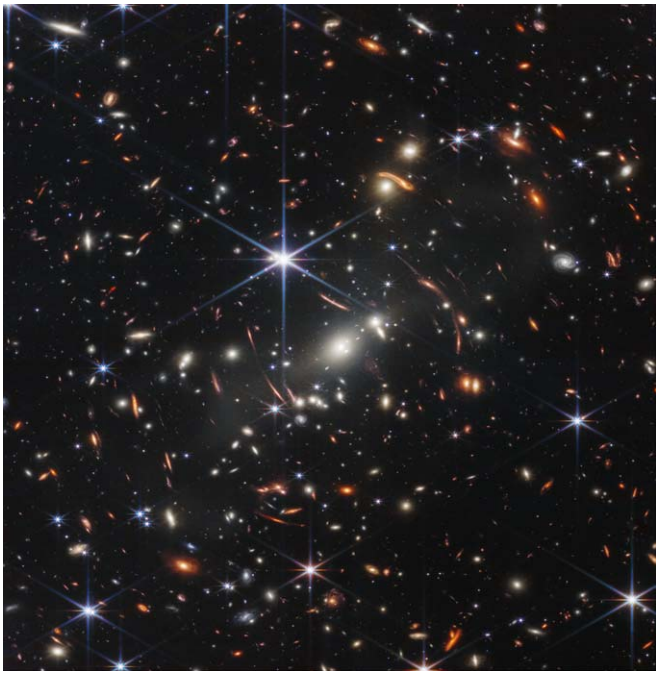

Figure 4. JWST's first released image, the lensing cluster SMACS 0723, which was the deepest infrared image ever taken.

Observing time on JWST is allocated by wall-clock time. All overheads are included in the time allocated. Overheads that are determined by the observing sequence, such as slews or mechanism movements, are accounted by the planning software. Overheads that are independent of the specific observations, such as the calibration program or station-keeping maneuvers, are accounted by a percentage of time applied to each program.

The Cycle 1 GO program was allocated approximately 6000 hr. Between the GTO, DD, and GO programs, the total number of hours in Cycle 1 exceeds 1 yr (8760 hr) by about 25%. The field of regard of JWST is about 40% of the sky at any given time. There will need to be enough targets within the field of regard at the end of Cycle 1 to efficiently schedule the observations, and the extra 25% tail will ensure a smooth transition from the end of Cycle 1 to the beginning of Cycle 2. The remaining allocated Cycle 1 observations will be conducted during the early months of Cycle 2, and there will be a similar transition from Cycle 2 to Cycle 3.

3.1. Director's Discretionary Early Release Observation Programs

The DD-ERS program consists of 13 programs, ranging from the early universe to our solar system. Collectively the programs use most of the JWST instrument modes. The data taken have no exclusive access period. Consequently, prior to writing Cycle 2 observing proposals, the scientific community were able to obtain JWST data from the archive that is relevant to their proposals. In this section, we describe the DD-ERS programs and report on those that had early scientific results that were published or submitted by 2022 September 30.

Table 2
GTO Allocations

Team	PI	Original	Current	Remaining	Executed
MIRI STScI	Christine Chen	12.0	10.5	1.5	0.0
NIRISS Team	Rene Doyon	450.0	469.2	6.9	34.9
NIRSpec Team	Pierre Ferruit	900.0	829.8	59.4	57.2
MIRI STScI	Scott Friedman	12.0	15.5	0.9	0.0
MIRI STScI	Karl Gordon	12.0	0.0	0.0	0.0
MIRI US	Thomas Greene	60.0	75.0	0.2	15.8
IDS	Heidi Hammel	110.0	141.5	1.0	32.7
MIRI STScI	Dean Hines	12.0	15.8	0.1	1.3
IDS	Simon Lilly	110.0	115.9	0.1	18.6
IDS	Jonathan Lunine	110.0	110.5	2.0	39.4
IDS	Mark McCaughrean	110.0	100.4	33.3	12.0
MIRI US	Margaret Meixner	60.0	76.2	0.3	26.6
Telescope Scientist	Matt Mountain	210.0	212.9	10.4	9.5
MIRI STScI	Alberto Noriega-Crespo	12.0	10.7	0.1	0.0
MIRI US	Michael Ressler	60.0	63.5	0.7	2.4
MIRI Science Lead	George Rieke	210.0	183.1	39.2	0.0
NIRCam Team	Marcia Rieke	900.0	1041.2	−3.9	108.3
IDS	Massimo Stiavelli	110.0	110.0	25.7	5.1
IDS	Rogier Windhorst	110.0	122.0	0.2	23.4
MIRI Europe	Gillian Wright	450.0	452.0	18.0	62.9
Totals		4020.0	4155.7	196.1	449.8

Note. The time allocations to GTO teams in hours. IDS stands for Interdisciplinary Scientist on the Science Working Group. The original allocations to each team (as set by policy and international agreements) have been modified due to exchanges or collaborations between GTO teams, and also due to changes in overhead calculations since the original programs were submitted. The column labeled "Remaining" refers to the number of hours remaining to be allocated in Cycle 2 or Cycle 3. The number of hours in the final column are those that have been executed by 2022 September 30. The current values of the information listed in this table are available from https://www.stsci.edu/cgi-bin/get-jwst-gto-time.

3.1.1. DD-ERS 1288; PDRs4All: Radiative Feedback from Massive Stars

Massive stars produce intense winds and radiation, which ionizes and heats the surrounding molecular cloud material, affecting future star formation in the cloud. These interactions create Photo-Dissociation Regions (PDRs), which dominate the infrared spectra of star-forming galaxies and drive the evolution of star formation from interstellar matter. PDRs4All (Berné et al. 2022) consists of NIRCam and MIRI imaging, and MIRI MRS and NIRSpec IFU spectroscopy of PDRs in the Orion Bar.

3.1.2. DD-ERS 1309; IceAge: Chemical Evolution of Ices During Star Formation

Icy grain mantles hold volatile elements and prebiotic complex organic molecules in star-forming regions. IceAge (McClure et al. 2018; McClure 2022) will use NIRSpec and MIRI spectroscopy and NIRCam wide-field slitless spectroscopy to study ice chemistry in a representative low-mass star-forming region at several stages: prestellar core, Class 0 protostar, Class I protostar, and protoplanetary disk. This program will map the spatial distribution of ices to 20–50 au. If the organic molecules survive the protostellar infall intact, then the molecular cloud could provide the precursors of biomolecules to the planetary systems that form within it. This could mean that life is a common outcome of star and planetary system formation.

3.1.3. DD-ERS 1324; Through the Looking GLASS: a JWST Exploration of Galaxy Formation and Evolution from Cosmic Dawn to Present Day

Gravitational lensing by a Frontier Field cluster allows JWST to reach intrinsically faint galaxies in the epoch of reionization. GLASS (Treu et al. 2022) will observe A2744 with NIRSpec multi-object spectroscopy and NIRISS wide-field slitless spectroscopy, and will also create a parallel deep field with NIRCam imaging. The parallel field will contain the deepest extragalactic data of the DD-ERS program. The spectroscopy will also be the deepest DD-ERS data obtained in those modes.

GLASS will identify galaxies within the epoch of reionization, and measure Lyα velocities and morphologies, rest-frame UV and optical emission line fluxes, and UV/optical photometry and sizes. The program will map metallicity, and the dust quantities and star formation rate for galaxies spanning log $M_\star \sim 6$ to 10 at $z > 2$, which was when disks and bulges emerged and feedback was most active. The GLASS NIRISS observations will map systems at $z < 3.5$ and log $M_\star \gtrsim 6$. The higher resolution NIRSpec observations will spectrally resolve key diagnostic lines ,which are blended at the lower resolution of the grism spectra. NIRSpec will also reach beyond $z \gtrsim 4$ galaxies.

The NIRCam parallel observations will cover $\sim$18arcmin^2 in two regions. They will use seven broad-band filters from F090W to F444W, and will reach 5σ limits of 29.2–29.7 AB magnitudes (according to the prelaunch exposure time calculator.)

The GLASS team has published a series of papers with initial results, and other groups have also used these public data. The GLASS team papers include: (1) lensed galaxies at $z > 7$ (Roberts-Borsani et al. 2022), (2) photometry and catalogs (Merlin et al. 2022), (3) galaxies at $z > 9$ (Castellano et al. 2022), (4) metallicity in low-mass galaxies at $z \sim 3$ (Wang et al. 2022), (5) the size–luminosity relation at $z > 7$ (Yang et al. 2022), (6) measurements of rest-frame optical lines (Boyett et al. 2022), (7) globular clusters at $z \sim 4$

Table 3
DD-ERS Programs

ID	Acronym	Title	PI and Co-PIs	Instruments
1288	PDRs4All	Radiative Feedback from Massive Stars as Traced by Multiband Imaging and Spectroscopic Mosaics	Olivier Berne, Emilie Habart, Els Peeters	M, NC, NS
1309	IceAge	IceAge: Chemical Evolution of Ices during Star Formation	Melissa McClure, Abraham C. Boogert, Harold Linnartz	M, NC, NS
1324	GLASS	Through the Looking GLASS: A JWST Exploration of Galaxy Formation and Evolution from Cosmic Dawn to Present Day	Tommaso Treu	NC, NI, NS
1328	GOALS-JWST	A JWST Study of the Starburst-AGN Connection in Merging LIRGs	Lee Armus, Aaron Evans	M, NC, NS
1334		The Resolved Stellar Populations Early Release Science Program	Daniel Weisz	NC, NI
1335	Q-3D	Q-3D: Imaging Spectroscopy of Quasar Hosts with JWST Analyzed with a Powerful New PSF Decomposition and Spectral Analysis Package	Dominika Wylezalek, Sylvain Veilleux, Nadia Zakamska	M, NS
1345	CEERS	The Cosmic Evolution Early Release Science (CEERS) Survey	Steven Finkelstein	M, NC, NS
1349	WR DustERS	Establishing Extreme Dynamic Range with JWST: Decoding Smoke Signals in the Glare of a Wolf–Rayet Binary	Ryan Lau	M, NI
1355	TEMPLATES	TEMPLATES: Targeting Extremely Magnified Panchromatic Lensed Arcs and Their Extended Star Formation	Jane Rigby, Joaquin Vieira	M, NC, NS
1364		Nuclear Dynamics of a Nearby Seyfert with NIRSpec Integral Field Spectroscopy	Misty Bentz	NS
1366		The Transiting Exoplanet Community Early Release Science Program	Natalie Batalha, Jacob Bean, Kevin Stevenson	M, NC, NI, NS
1373		ERS Observations of the Jovian System as a Demonstration of JWST's Capabilities for Solar System Science	Imke de Pater, Thierry Fouchet	M, NC, NI, NS
1386		High Contrast Imaging of Exoplanets and Exoplanetary Systems with JWST	Sasha Hinkley, Andrew Skemer, Beth Biller	M, NC, NI, NS

Note. The 13 selected Director's Discretionary Early Release Science Programs. Instruments: NC = NIRCam, NI = NIRISS, NS = NIRSpec, M = MIRI.

(Vanzella et al. 2022), (8) the detection of a lensed star at $z = 2.65$ (Chen et al. 2022b), (9) spectra of low-mass galaxies at $z \gtrsim 2$ (Marchesini et al. 2023), (10) measurements of the rest-frame UV at $7 < z < 9$ (Leethochawalit et al. 2022), (11) masses and M/L at $z > 7$ (Santini et al. 2023), (12) the morphology of high-z galaxies (Treu et al. 2023), (13) faint cold brown dwarfs (Nonino et al. 2023), (14) a morphological atlas at $1 < z < 5$ (Jacobs et al. 2023), (15) faint high-z sources are intrinsically blue (Glazebrook et al. 2023), (16) UV slopes at $4 < z < 7$ (Nanayakkara et al. 2023), and (17) star formation histories at $5 < z < 7$ (Dressler et al. 2023).

Other results from the GLASS observations include a lensing model of A2722 (Bergamini et al. 2023) and two studies using ALMA data of $z > 12$ candidates (Bakx et al. 2023; Popping 2023).

3.1.4. DD-ERS 1328; A JWST Study of the Starburst-AGN Connection in Merging LIRGs

Luminous Infrared Galaxies (LIRGs) are some of the most active regions of star formation in the universe. The connection between starbursts and Active Galactic Nuclei (AGN), and the role of galaxy merging in feeding both the star formation and supermassive black hole growth, has implications for both feedback and the star formation history of the universe. Program 1328 (e.g., Lai et al. 2022) will obtain NIRSpec and MIRI IFU spectroscopy, along with NIRCam and MIRI imaging, of active galaxies taken from the Great Observatories All-Sky LIRG Survey (Armus et al. 2009, GOALS).

Initial results from GOALS-JWST include detection of an AGN-driven outflow from the nucleus of NGC 7469 using mid-infrared spectroscopy (Armus et al. 2023), and a map of the Polycyclic Aromatic Hydrocarbon (PAH), molecular gas emission (Lai et al. 2022), and ionization states (U et al 2022) in the object. NIRCam and MIRI imaging of NGC 7469 show star-forming regions that are consistent with young (<5 Myr) stellar populations, showing an age bimodality in the star-forming regions of the ring (Bohn et al. 2023). GOALS-JWST observations of the merger VV114 resolved its double nuclei and showed that the southwestern core had AGN-like colors, while the northeastern core was a starburst (Evans et al. 2022). About half of the mid-infrared emission in the object was diffuse, including PAH emission. Observations of the merging galaxy IIZw096 showed that between 40% and 70% of the infrared bolometric luminosity came from a single region smaller than 175 pc in radius (Inami et al. 2022).

3.1.5. DD-ERS 1334; The Resolved Stellar Populations Early Release Science Program

The Resolved Stellar Populations DD-ERS program (Gilbert et al. 2018; Weisz et al. 2023) will observe the globular cluster M92, the ultra-faint dwarf Draco II and the star-forming dwarf WLM to measure the subSolar mass stellar initial mass function (IMF), extinction maps, evolved stars, proper motions, and globular clusters. The program will use NIRCam imaging with NIRISS imaging in parallel, both using the F090W and F150W filters, with either wide or medium-band filters in the long-wavelength NIRCam channel. The program will also develop point-spread-function-fitting software specific to NIRCam and NIRISS for evaluating crowded stellar populations (Warfield et al. 2023).

Early results from Program 1334 include color–magnitude diagrams of M92, reaching almost to the bottom of the M92 main sequence ($\sim 0.1 M_{\odot}$), and finding white dwarf candidate members of M92 in the brightest portion of the white dwarf cooling sequence (Nardiello et al. 2022).

3.1.6. DD-ERS 1335; Q-3D: Imaging Spectroscopy of Quasar Hosts with JWST Analyzed with a Powerful New PSF Decomposition and Spectral Analysis Package

The Q-3D program uses NIRSpec and MIRI IFU observations of luminous quasars as templates to develop a PSF decomposition and spectral analysis packages, separating the bright central quasar from the host galaxy extended emission (Wylezalek 2022). This program will measure the stellar, gas, and dust components to determine the impact of luminous quasars on their hosts. It will observe three systems: F2M1106, XID2028, and SDSSJ1652.

3.1.7. DD-ERS 1345; The Cosmic Evolution Early Release Science (CEERS) Survey

The statistical study of galaxy formation and evolution through deep-field observations with Hubble, Spitzer, Chandra and many other facilities has a rich history, including the Hubble Deep Field (Williams et al. 1996), the Great Observatories Origins Deep Survey (Giavalisco et al. 2004), the Hubble Ultra-Deep Field (Beckwith et al. 2006), the Cosmic Assembly Near-infrared Deep Extragalactic Legacy Survey (CANDELS, Grogin et al. 2011; Koekemoer et al. 2011), the Frontier Fields (Lotz et al. 2017) and many others. The CEERS survey will image 100 arcmin^2 within the CANDELS Extended Groth Strip field with NIRCam and MIRI. This program will obtain NIRSpec MSA and NIRCam WFSS spectroscopy of objects detected in the imaging. The science goals of CEERS includes finding galaxies at $z > 9$, constraining their nature and abundance, obtaining spectra of galaxies at $z > 3$, including candidates at $z > 6$, and characterizing the MIR emission from galaxies to study dust-obscured star formation and supermassive black hole growth.

Early results from the CEERS data include the discovery of candidate galaxies at $z > 8$ (e.g., Finkelstein et al. 2022; Naidu et al. 2022; Topping et al. 2022; Ono et al. 2022) and studies of galaxies at $3 < z < 7$, including quiescent galaxies (Carnall et al. 2023), AGN host galaxies (Ding et al. 2022; Kocevski et al. 2023; Onoue et al. 2023), star-forming clumps (Chen et al. 2023), and sources detected at other wavelengths (e.g., Chen et al. 2022a).

3.1.8. DD-ERS 1349; Establishing Extreme Dynamic Range with JWST: Decoding Smoke Signals in the Glare of a Wolf–Rayet Binary

Colliding-wind Wolf–Rayet (WR) binaries efficiently produce dust and are important sources for the production of dust in galaxy evolution. WR DustERS (Lau & WR DustERS Team 2022) will observe two carbon-rich WR systems; WR-140 is the archetypal colliding-wind binary, while WR-137 is a known periodic dust-maker (Lau et al. 2020). This program will obtain the first resolved mid-infrared spectrum of the dust around a carbon-rich WR star, using MIRI IFU and imaging. They will develop PSF-subtraction techniques that are useful for observing faint extended emission around bright sources in IFU data sets. The observations of WR-137 will be done with

NIRISS AMI mode to detect the faint dust spiral around the bright central source.

MIRI imaging of WR-140 detected 17 nested dust shells, which formed at each periastron 7.93 yr apart over the past 130 yr. Understanding the chemical properties and spectral signatures of dust formed by binaries such as WR-140 is important given their potential role as dust sources in the interstellar medium. MIRI spectroscopy of the second dust shell confirmed the survival of carbonaceous dust grains seen as PAH features and are consistent with a composition of carbon-rich aromatic compounds in a hydrogen-poor environment. Since this carbonaceous dust has lasted for at least 130 yr in the harsh radiation environment of the central binary system, it could be a possible early and potentially dominant source of organic compounds and dust in the ISM of our galaxy (Lau & WR DustERS Team 2022).

3.1.9. DD-ERS 1355; TEMPLATES: Targeting Extremely Magnified Panchromatic Lensed Arcs and Their Extended Star formation

Objects that are magnified by gravitational lensing can be observed with greater intrinsic spatial resolution and higher sensitivity. TEMPLATES (Rigby & Templates Team 2020) will obtain NIRSpec and MIRI IFU spectroscopy and imaging of four gravitationally lensed galaxies selected at $1 < z < 4$. This program will spatially resolve star formation structures in an extinction-robust manner, mapping Hα, Paα and 3.3 μm PAH features within the galaxies. The selected targets are the brightest and best-characterized lensed systems known.

3.1.10. DD-ERS 1364; Nuclear Dynamics of a Nearby Seyfert with NIRSpec Integral Field Spectroscopy

Measuring the mass of a supermassive black hole in a galaxy can be done with dynamical measurements or with reverberation mapping. It is important to connect dynamical measurements, primarily done on local quiescent galaxies, to reverberation mapping of more distant active galaxies. Program 1364 will use NIRSpec IFU observations of NGC 4151 to directly measure the mass of the central black hole and make a comparison to the previous reverberation mapping measurements of the same object (Bentz et al. 2022). This program will measure kinematic maps of the stars and gas, intensity maps of the gas, and stellar dynamical models of the galaxy.

3.1.11. DD-ERS 1366; The Transiting Exoplanet Community Early Release Science Program

Transiting exoplanets will allow JWST to measure atmospheric compositions, structures, and dynamics in unprecedented detail. Program 1366 will use time-series observations in all four instruments to observe WASP-39b in transit, a MIR phase curve of WASP-43b, and a secondary eclipse of WASP-18b.

Early results include the first clear detection of CO_2 at 4.3 μm in an exoplanet, WASP-39b (JWST Transiting Exoplanet Community Early Release Science Team et al. 2023). The observations were made with the NIRSpec bright object time sequence mode and the $1\farcs6 \times 1\farcs6$ fixed slit aperture. A total of 21,500 integrations over 8.23 hr included the 2.8 hr transit duration.

3.1.12. DD-ERS 1373; ERS observations of the Jovian System as a Demonstration of JWST's Capabilities for Solar System Science

JWST enables solar system observations with moving-target tracking and several modes optimized for bright targets. The prelaunch moving-target tracking requirement was 30 mas s^{-1}, but the telescope managed to track the Double Asteroid Redirection Test (DART) impact on P/Didymos on 2022 September 26 at a rate of 105 mas s^{-1}. Program 1373 is an in-depth study of the Jovian system that will characterize Jupiter's cloud layers, winds, composition, auroral activity and temperature structure; map Io and Ganymede; and characterize Jupiter's ring structure. This program uses all four instruments.

3.1.13. DD-ERS 1386: High Contrast Imaging of Exoplanets and Exoplanetary Systems

The direct characterization of exoplanets with JWST will enable mid-infrared coronagraphy and detailed spectroscopy for the first time. Program 1386 (Hinkley et al. 2022) will use all four instruments to characterize two exoplanets and a circumstellar disk in the NIR and MIR. Early results include NIRCam and MIRI coronagraphic imaging of the super-Jupiter exoplanet HIP 65426b from 2 μm to 16 μm (Carter et al. 2022), which is the first direct detection of an exoplanet at wavelengths longer than 5 μm. The observations are fitted by a mass of 7.4 ± 1.1 $M_{\rm Jup}$. Miles et al. (2023) presented the highest fidelity spectrum to date of a planetary-mass object, VHS 1256 b, which is a $<20 M_{\rm Jup}$, widely separated, young brown dwarf companion. Water, methane, carbon monoxide, carbon dioxide, sodium, and potassium were observed in the JWST spectra, which indicate disequilibrium chemistry and clouds. The authors made a direct detection of silicate clouds for the first time in a planetary-mass companion.

4. Mission Design

The JWST mission consists of an observatory, a ground system provided by Space Telescope Science Institute, and launch services provided by Arianespace under the direction of ESA. The observatory includes all the on-orbit hardware. The prime contractor for the observatory was Northrop Grumman Aerospace Systems (NGAS). The observatory consists of an optical telescope element that was provided by Ball Aerospace, a spacecraft and sunshield provided by NGAS, and an Integrated Science Instrument Module (ISIM) constructed by Goddard Space Flight Center. The ISIM houses the four science instruments and provides them with thermal, electrical, structural, and data handling support.

The Near-Infrared Camera (NIRCam; Rieke et al. 2023, this issue) was built by Lockheed Martin under the direction of Principal Investigator Marcia Rieke of the University of Arizona. All of the near-infrared instruments include detectors from Teledyne Imaging Systems. The Near-Infrared Spectrograph (NIRSpec; Böker et al. 2023, this issue) was built by EADS Astrium under the direction of ESA, and includes a microshutter assembly (MSA) and detector system built by Goddard Space Flight Center. The Near-Infrared Imager and Slitless Spectrograph (NIRISS Doyon et al. 2023, this issue) was built by Honeywell under the direction of CSA. The Fine Guidance System (FGS) is included with the NIRISS and shares the same optical bench. The MIRI (Wright et al. 2023, this issue) consists of an optical bench assembly built by a consortium of European countries organized by ESA, a

cryocooler built by Northrop Grumman under the direction of Jet Propulsion Laboratories, and a detector system by JPL and Raytheon Intelligence & Space.

The mission design and its performance is summarized here. Details provided about the telescope are given by McElwain et al. (2023), (this issue); construction, integration, and test of the observatory by Menzel et al. (2023), (this issue); the on-orbit performance measured during commissioning by Rigby et al. (2023a), (this issue); and the on-orbit backgrounds measured during commissioning by Rigby et al. (2023b), (this issue).

4.1. Launch, Orbit, Deployments, and Commissioning

The JWST observatory was launched from Centre Spatial Guyanais at 12:20 UTC on 2021 December 25 by an Ariane 5 ECA+ rocket. The launch mass was 6161.4 kg. The launch provided a near-perfect trajectory. Three mid-course correction (MCC) burns placed the observatory in an L2 halo orbit, approximately 1.5×10^6 km from Earth. The successful launch and MCC burns used less on-board fuel than allocated—the remaining propellant will enable a fuel-limited lifetime of more than 20 yr.

Launch was followed by more than 50 major deployments, which were completed successfully enroute to the final orbit. The major deployed systems included the solar panel, the high-gain antenna, the deployed tower assembly, the sunshield, the secondary mirror, an instrument radiator, and the primary mirror wings. The sunshield deployment included 140 membrane release mechanisms, 70 hinge assemblies, 8 deployment motors, 400 pullies, and 90 cables totaling more than 400 m. Following the major deployments, which were completed in the first 14 days, the primary mirror segments and secondary mirror were moved off their launch locks.

At the completion of the deployments, the telescope was pointed at HD 84406 (Gaia Collaboration et al. 2018) to begin the telescope alignment and phasing process. The major steps included: (1) segment image identification, (2) segment alignment, (3) image stacking, (4) coarse phasing, (5) fine phasing, (6) telescope alignment over instrument fields of view, and (7) iterate alignment for final correction. Following telescope alignment, commissioning of the instruments included activating all of the instrument systems and commissioning the 17 science instrument modes. The final commissioning tasks included taking the Early Release Observations (ERO). Commissioning was completed by 2022 July 11 and 12 with the release of the EROs.

4.2. Optical Telescope Element

The optical telescope element (OTE) consists of a primary mirror that is made up of 18 hexagonal beryllium primary mirror segment assemblies (PMSAs), a 0.8 m convex secondary mirror, and an aft optical assembly subsystem containing a tertiary mirror and a fine-steering mirror. All of the mirrors are coated with gold. The PMSAs and secondary mirror were aligned and phased on-orbit using actuators that had a total of 132 degrees of freedom. The total collecting area of the primary mirror is 25.4 m^2, as measured on-orbit using the NIRCam pupil imaging lens. The telescope was designed to be diffraction-limited at 2 μm wavelength, defined as having a Strehl ratio >0.8 (Bely 2003) at the end of a 5 yr post-commissioning lifetime, equivalent to 150 nm, root-mean squared (rms) wave front error (WFE). The WFE at the end of commissioning was ~80 nm rms, which is equivalent to a diffraction limit at 1.1 μm. The expected degradation of the wave front error due to micrometeoroid impacts and other effects over the operational lifetime of the mission will be closely monitored (Rigby et al. 2023a; McElwain et al. 2023, this issue).

4.3. Spacecraft

The spacecraft provides power, pointing, orbit maintenance, data storage, and communications for the observatory. At the end of commissioning, the solar array provided an average of 1.5 kW of power, with the ability to provide 3 kW when needed. The pointing system uses star trackers, inertial reference units (IRUs) containing gyros, reaction wheels, and a fine-steering mirror (FSM) to point the telescope. There are three star trackers, one of which provides redundancy. There are two IRUs, one of which is redundant; each IRU includes four gyros, one of which provides redundancy. There are six reaction wheels, of which two provide redundancy. The star trackers, gyros and reaction wheels maintain the attitude and coarse pointing of the observatory. During fine guiding, after guide star acquisition, the FGS provides a 16 Hz positional update to the fine-steering mirror to adjust the pointing of the telescope. At the end of commissioning, the pointing system delivers pointing stability of ~1.5 mas (1σ per axis), which greatly exceeds the prelaunch requirement of 4 mas. Orbit maintenance currently requires the on-board thrusters to be fired about once every 6 weeks. The thruster firings are also used to maintain angular momentum by de-spinning the reaction wheels. The frequency of orbit maintenance and angular momentum management is determined through ranging measurements and reaction wheel telemetry.

The on-board solid-state recorder holds 471 Gbits of science and engineering data. The data are downlinked via Ka band through the Deep Space Network (DSN) on a nominal schedule of two contacts per day, totaling up to 12 hr. The actual downlink schedule varies from day to day, depending on which antenna is in range and DSN scheduling with respect to other mission needs. Commands and observation plans are uplinked to the observatory through the DSN using *S* band.

4.4. Sunshield and Cooling

The sunshield consists of five layers of Kapton, about 14 m × 22 m in size, that separate the ~300 K spacecraft from the telescope, and attenuate the ~200 kW of incident Solar radiation to mW levels. The sunshield's size and geometry provides an instantaneous field of regard of 40% of the sky in an annulus that sweeps around the full sky once per year. Each point on the sky is visible at least once in each six-month period. The telescope can point 5° toward the Sun and 45° away from the Sun, and can spin around the Sun-anti-Sun axis.

Immediately after launch, the observatory began passively cooling. This process that was completed within 120 days. The cooldown was controlled using heaters to ensure that the instruments would not be contaminated by condensation of outgassing water and other volatiles. The MIRI cryocooler (the only active cooling in the observatory) was turned on after the deployments and reached its final temperature on day 104. The final temperature reached by the secondary mirror is 29.2 K. The primary mirror segments range from 34.7 to 54.5 K. The

Table 4
Science Instrument Characteristics

Instrument	Wavelength (μm)	Detector	Plate Scale (mas/pix)	Field of View
NIRCam				
short	0.6–2.3	Eight 2048 × 2048	32	2′.2 × 4′.4
long[a]	2.4–5.0	Two 2048 × 2048	65	2′.2 × 4′.4
NIRSpec	0.6–5.0	Two 2048 × 2048	100	
MSA[b]				3′.4 × 3′.1
slits[c]				∼200″ mas × 4″
IFU				3″.0 × 3″.0
MIRI				
imaging	5–27	1024 × 1024	110	1′.4 × 1′.9
spectra[d]	5–10			26″ × 26″
IFU	5–28	Two 1024 × 1024	200–470	3″.6 × 3″.6 to 7″.5 × 7″.5
NIRISS		2048 × 2048	65	2′.2 × 2′.2
imaging	0.6–5.0			
WFSS	0.8–2.2			
SOSS	0.6–2.8			
AMI	2.8–4.8			
FGS	0.6–5.0	Two 2048 × 2048	65	2′.2 × 4′.4

Note. (a) Use of a dichroic renders the NIRCam long-wavelength field of view co-spatial with the short-wavelength channel and the two channels acquire data simultaneously. (b) NIRSpec includes a microshutter assembly (MSA) with four 384 × 175 microshutter arrays. The individual shutters are each 250 (spectral) × 500 (spatial) mas. (c) NIRSpec also includes several fixed slits which provide redundancy and high-contrast spectroscopy on individual targets, and an IFU. (d) MIRI includes a fixed slit for low-resolution ($R \sim 100$) spectroscopy over the 5–10 μm range, and an IFU for $R \sim 3000$ spectroscopy over the full 5–28 μm range. The long-wavelength cut-off for MIRI spectroscopy is set by the detector performance, which drops beyond 28.0 μm.

mirror segments that are closest to the core region near the sunshield at the bottom of the telescope are warmer than the mirror segments at the top and wings. With these temperatures, JWST broad-band observations are background limited by zodiacal light out to about 12.5 μm wavelength, and limited by thermal self-emission at longer wavelengths (Rigby et al. 2023b, this issue). The near-infrared instrument detector plane temperatures are actively maintained using heaters at 38.5 K for NIRCam and NIRISS, and 42.8 K for NIRSpec. The MIRI optical assembly is kept at 6 K by the cryocooler, while the MIRI shield around the instrument is about 20 K.

5. Instruments

JWST has four science instruments with a total of 17 science instrument modes (see Table 4). All of the instrument capabilities expected before launch have been enabled and are in use. Almost all of the instrument requirements have been exceeded; in particular most of the instrument modes are more sensitive than the prelaunch expectations, and the point-spread function at the shorter wavelengths is sharper than the prelaunch expectations.

5.1. NIRCam

NIRCam (Rieke et al. 2003; Horner & Rieke 2004; Rieke et al. 2023, this issue) provides imaging from 0.6 to 5.0 μm in broad-band, medium-band and narrow-band filters. It has a wide-field slitless spectroscopy capability from 2.5 to 5.0 μm. It has a coronagraphic mode. NIRCam is designed with two modules observing parallel fields of view. Each module contains a dichroic at 2.4 μm to provide simultaneous data in two filters longward and shortward of the dichroic. The two modules are identical, including the wave front sensing hardware, and provide full redundancy in case of failure. The total field of view is 2.2 × 4.4 arcmin^2, and there are a total of 10 detectors, with eight in the short-wavelength channel and two in the long-wavelength channel. All of the near-infrared instruments (NIRCam, NIRSpec, NIRISS, and FGS) use H2RG HgCdTe 2048 × 2048 focal-plane arrays made by Teledyne Imaging Systems (e.g., Rauscher et al. 2014). The NIRCam plate scales are 32 mas per pixel in the short-wavelength channels and 65 mas per pixel in the long-wavelength channels, Nyquist sampling the diffraction limit at 2.0 μm and 4.0 μm, respectively. NIRCam also functions as part of the wave front sensing and control system.

5.1.1. NIRCam Imaging

NIRCam contains two extra-wide filters, eight broad-band filters, 12 medium-band filters and seven narrow-band filters. The broad-band filters span the full wavelength range of the instrument, the extra-wide and medium-band filters cover 1.0 μm to 4.0 μm and 1.4 μm to 5.0 μm respectively, and the narrow-band filters are selected to match individual spectral lines. NIRCam imaging sensitivity exceeds the prelaunch expectations in almost all of the filters. The requirements were 11.4nJy and 13.8nJy at 2.0 μm and 3.5 μm, point-source sensitivity, 10σ in 10,000 s. The sensitivity at the end of commissioning were 7.3nJy and 8.8nJy, respectively. NIRCam imaging is one of the most-used modes in Cycle 1 programs. An example that uses this mode can be found in Program 1963, which is a medium-band survey of the Hubble Ultra-Deep Field.

5.1.2. NIRCam Wide-field Slitless Spectroscopy

NIRCam wide-field slitless spectroscopy (WFSS; Greene et al. 2017) provides $R \sim 1600$ spectra of all of the objects within the field of view using a grism. The grism is used in the long-wavelength channel in combination with a wide or medium filter to provide spectroscopy in the 2.5–5.0 μm wavelength range. Short wavelength <2.5 μm imaging in the short-wavelength channel can be taken simultaneously with the WFSS measurements. Commissioning data show that the total throughput is 20% to 40% higher than prelaunch expectations. An example that uses this mode can be found in Program 2078, searching for galaxies at the same redshift as $6.5 < z < 6.8$ quasars. Sun et al. (2022a, 2022b) discovered Hα+[O III] λ5007 line emitters at $z > 6$ using the NIRCam WFSS mode in commissioning data.

5.1.3. NIRCam Coronagraphy

NIRCam coronagraphy (Krist et al. 2009) has three round- and two bar-shaped coronagraphic masks for occulting a bright object. The inner working angles range from 0.″40 to 0.″81 for the round masks, corresponding to $6\lambda/D$ at 2.1 μm, 3.35 μm and 4.1 μm, and 0.″13 to 0.″88 for the bar masks. During a bar observation, the bright object is positioned behind the bar at the location where the IWA $\sim 4\lambda/D$. The masks are used in conjunction with a filter. Commissioning demonstrated that this mode provided a 5σ contrast at 1″ better than 4×10^{-5} (Girard et al. 2022). An example that uses this mode can be found in Program 1386, which is the DD-ERS high-contrast exoplanet imaging program (Carter et al. 2022; Hinkley et al. 2022).

5.1.4. NIRCam Bright Object Time Series: Imaging

Bright object time series (BOTS) observations are designed to measure photometric variations in relatively bright sources. NIRCam imaging BOTS uses rapid readout of subarrays, ranging from 64×64 to 160×160, in combination with filters or a weak lens, to increase the readout cadence and increase the saturation limits. Commissioning observations showed that the NIRCam BOTS imaging performance was nominal. An example that uses this mode can be found in Program 2635, which studies infrared emission of 4U0142 + 61. This is a magnetar with a possible silicate spectral feature at 9.7 μm, which has been interpreted as a passive disk surrounding the energetic isolated neutron star.

5.1.5. NIRCam Bright Object time Series: Grism

NIRCam grism BOTS observations provide $R \sim 1600$ spectroscopic observations of bright, isolated, time-varying sources. The spectroscopy in the long-wavelength channel is paired with weak lens observations in the short-wavelength channel to avoid saturation. This mode is capable of observing targets as bright as naked-eye stars (mag < 5). Commissioning observations of the transiting exoplanet HAT-P-14 b obtained a 91 ppm spectrum (when binned to $R = 100$). An example that uses this mode can be found in Program 2084, which searches for lava rain on the hot super-Earth planet 55 Cancri e.c

5.2. NIRSpec

NIRSpec (Jakobsen et al. 2022; Böker et al. 2023, this issue) provides spectroscopy from 0.6 to 5.3 μm at $R \sim 100$, $R \sim 1000$ and $R \sim 3000$ using fixed slits, a microshutter assembly (MSA) (Ferruit et al. 2022), or an IFU (Böker et al. 2022). The detector system consists of two Teledyne 2048×2048 H2RG arrays controlled and read by SIDECAR ASICs. The 18 μm × 18 μm pixels of the detector arrays project to an average of 0.″103 in the dispersion direction and 0.″105 in the spatial direction. Dispersion is done with a prism ($R = 30$–300) or gratings ($R = 500$–1343 or $R = 1321$–3690). The dispersion is crossed with filters to limit the bandwidth and resulting length of the spectra on the detectors. In most cases, the throughput of the instrument is higher than the prelaunch expectations.

5.2.1. NIRSpec Multi-object Spectroscopy

NIRSpec multi-object spectroscopy is done using the MSA, which is a MEMS assembly that consists of four quadrants. Each MSA slit is 0.″203 by 0.″463, with a ∼0.″07 wall between the openings. There are 730 (spectral) by 342 (spatial) pixels in the full array, spanning a field of view of approximately 3.′6 by 3.′4. The MSA is fully configurable, except for a limited number of failed slits. Typically, the MSA can be configured to observe up to 100 objects simultaneously, including sky subtraction, without overlapping spectra. Multi-object spectroscopy is one of the most highly used instrument modes in Cycle 1. An example of this can be found in Program 1345, the Cosmic Evolution Early Release Science (CEERS) Survey, which is a DD-ERS program that targets a deep field.

5.2.2. NIRSpec Fixed Slit Spectroscopy

NIRSpec has five fixed slits, which provide the highest contrast and throughput on individual targets for NIRSpec. The fixed slits also provide a redundant spectroscopic capability to the mission if the MSA mechanism were to fail. Three fixed slits are 0.″2 wide by 3.″3 long, and one is 0.″4 wide by 3″8 long. There is also a 1.″6 × 1.″6 high-throughput slit that is primarily used with the NIRSpec bright object time-series mode. An example of this can be found in Program 1936, which is a target of opportunity program that will target a kilonova detected by the LIGO/Virgo/KAGRA gravitational wave detectors during their Observing Run 4.

5.2.3. NIRSpec Integral Field Unit Spectroscopy

The IFU entrance aperture is a contiguous 3.″1 × 3.″2 field of view, divided into 30 slices totaling 900 spaxels, each 0.″103 × 0.″105. By providing a full spectral data cube, this mode gives the most complete information on a single target in the near-infrared with JWST. The throughput is slightly lower than prelaunch expectations in the red but higher in the blue. An example of this can be found in Program 1355, Targeting Extremely Magnified Panchromatic Lensed Arcs and Their Extended Star formation (TEMPLATES), which is a DD-ERS program that targets individual galaxies that are highly boosted by gravitational lensing.

5.2.4. NIRSpec Bright Object time Series

NIRSpec BOTS (Birkmann et al. 2022) primarily uses the 1.″6 × 1.″6 fixed slit, combined with detector subarrays of either 16 or 32 pixels wide, to rapidly monitor bright time-varying objects, such as observations of stars with transiting exoplanets. The readout cadence can be as fast as 0.28 s, potentially reaching stars brighter than $J < 6$ in some modes. During commissioning, the mode was tested on HAT-P-14 b and reached a noise level of <60 ppm (Espinoza et al. 2023). An example of this can be found in Program 2159, which follows a hot super-Earth-size exoplanet for a full orbit to map the planet's temperature.

5.3. NIRISS

NIRISS (Doyon et al. 2012, 2023, this issue) provides three specialized scientific capabilities and redundant broad-band imaging, over the wavelength range 0.7–5.0 μm. NIRISS is packaged with the FGS, which provides the signal to the fine-steering mirror and the attitude control system to lock onto targets and provide fine guiding. NIRISS has a field of view of 2.′2 × 2.′2, matching the FOV of one of the two NIRCam channels. NIRISS has a single 2048×2048 5 μm cut-off Hawaii-2RG detector, with 65 milliarcsec per pixel.

5.3.1. NIRISS Single Object Slitless Spectroscopy

NIRISS single-object slitless spectroscopy (SOSS; Albert et al. 2023) defocuses the telescope beam to spread the signal from bright objects over about 25 pixels to avoid saturation. SOSS provides medium-resolution spectroscopy ($R \sim 70$) between 0.6 and 2.8 μm. There are two usable orders. Using subarrays shortward of 1.0 μm allows targets as bright as $J = 6.5$ (Vega mag). An example of this can be found in Program 2589, where the SOSS mode will be used to detect and characterize the possible atmospheres of the small and rocky exoplanets TRAPPIST 1b and 1 c.

5.3.2. NIRISS Wide-field Slitless Spectroscopy

NIRISS wide-field slitless spectroscopy (WFSS) (Willott et al. 2022) enables low-resolution ($R \sim 150$) slitless spectroscopy over the $2\farcm2 \times 2\farcm2$ FOV at 0.8–2.2 μm wavelength. It is optimized to search for Lyα emitting galaxies during the epoch of reionization. It can also be used efficiently in parallel mode. Two orthogonal gratings provide dispersion in two directions to disentangle overlapping spectra and reduce confusion in crowded fields. The gratings are crossed with wide- or medium-band filters, which also reduces blending of the objects. Throughput of the WFSS mode exceeds the prelaunch expectations. An example of this can be found in Program 1571, PASSAGE—Parallel Application of Slitless Spectroscopy to Analyze Galaxy Evolution, which is a pure-parallel search for active star-forming galaxies.

5.3.3. NIRISS Aperture Masking Interferometry

NIRISS aperture masking interferometry (AMI; Sivaramakrishnan et al. 2012, 2023) uses a seven-aperture mask to enable high-contrast imaging at an inner working angles less than λ/D. AMI is used with the F380M, F430M, or F480M filters, and typically uses an 80×80 pixel subarray for bright sources. During commissioning, AMI was demonstrated by detecting AB Dor C, a companion separated by $\sim 0\farcs3$ with a contrast ratio of 4.5 mag (Kammerer et al. 2022). For example, the DD-ERS Program 1349, WR DustERS will observe the Wolf–Rayet binary WR 137 with AMI to investigate the dust abundance, composition, and production rates of dusty sources in the colliding winds of the stars.

5.3.4. NIRISS Imaging

NIRISS includes an imaging capability using a set of backup NIRCam broad-band filters and some medium-band filters. Since NIRISS imaging covers half the FOV of NIRCam, and does not include a dichroic, this mode is primarily for imaging redundancy in the mission. NIRISS imaging can also be used in parallel to NIRCam imaging for additional areal coverage, and is used in support of WFSS data. Program 2561, which will observe the Frontier Field lensing cluster A2744, uses NIRISS imaging in parallel to NIRCam imaging to increase the area of deep photometric studies of high-redshift galaxies at mild lensing magnifications.

5.4. MIRI

MIRI (Rieke et al. 2015a; Wright et al. 2015, 2023, this issue) provides both imaging in broad-band filters and IFU spectroscopy from 5.0 to 28.0 μm. It also has low-resolution slit spectroscopy from 5.0 to 12.0 μm (where the sensitivity is limited by the zodiacal light background) and a coronagraphic capability. MIRI has three arsenic-doped silicon (SI:As) impurity band conduction detector arrays, each of 1024×1024 pixel format with 25 μm pixel pitch, made by Raytheon Intelligence & Space (Ressler et al. 2015; Rieke et al. 2015b). The plate scale is 110 mas per pixel, which Nyquist samples the point-spread function at 6.25 μm. Two of the detectors are used for the medium-resolution spectroscopy, while the third is used for imaging, low-resolution spectroscopy, and coronagraphy. The MIRI instrument is actively cooled to an operating temperature of 6.0 K with a $\sim$6 K/18 K hybrid mechanical cooler, which was developed by Northrop Grumman in collaboration with JPL. The MIRI cooler uses gaseous helium as the coolant. There is a three stage pulse-tube precooler, which reaches $\sim$18 K and a fourth $\sim$6 K Joule-Thompson cooler stage. The cooler compressor is in the JWST spacecraft bus at room temperature, while the cold head assembly cooling the instrument is on the ISIM structure.

5.4.1. MIRI Imaging

MIRI imaging (Bouchet et al. 2015) uses nine broad-band filters to cover the 5–27 μm wavelength region. The imaging field of view is 1.4×1.9 arcmin^2 sampled with $0\farcs11$ pixels. (The remaining field of view of the detector is occupied by the coronagraphs and the low-resolution spectrometer.) MIRI imaging can use subarray readouts for bright objects that would saturate in a full frame, observing objects as bright as 0.1 Jy in the F560W filter (Glasse et al. 2015). An example that uses this mode can be found in Program 2130, which will observe several square kpc in three nearby galaxies—M33, NGC 300, and NGC 7793—to measure dust-enshrouded stellar populations.

5.4.2. MIRI Low-resolution Spectroscopy

MIRI low-resolution spectroscopy (LRS; Kendrew et al. 2015) provides $R \sim 100$ long-slit and slitless spectroscopy from 5 to 12 μm, the MIR wavelength range where JWST observations are still zodiacal-light limited. A slit mask is permanently in the field of view. Slitless spectroscopy is available anywhere within the imager's field of view when the $R \sim 100$ double prism assembly is selected in the imaging filter wheel. For bright sources, a subarray readout can be used. In practice, the source will be placed in a dedicated LRS slitless detector region and read out in a subarray. It is expected that most LRS slitless targets will be bright nearby stars with transiting planets to obtain spectra of exoplanet atmospheres. Program 1658 will observe Pluto's moon Charon using the MIRI LRS mode.

5.4.3. MIRI Medium-resolution Spectroscopy

MIRI medium-resolution spectroscopy (MRS Wells et al. 2015) provides integral-field spectroscopy over the full 5 μm to 28 μm MIRI wavelength range. The spectral resolution ranges from $\sim$3300 at the short-wavelength end to $\sim$1300 at the longest wavelengths. There are four channels separated in wavelength by dichronics, with between 12 and 21 image slices. Depending on wavelength, the field of view ranges from $3\farcs70 \times 3\farcs70''$ to $7\farcs74 \times 7\farcs95$. Each individual exposure provides two wavelength ranges on two detectors, and three exposures are required to get a full wavelength spectrum. MIRI MRS is used in many programs; for example, Program 1549 will observe three molecule-rich protoplanetary disks that were

shown to have very bright water line emissions in Spitzer spectra.

5.4.4. MIRI Coronagraphic Imaging

The imaging channel on MIRI includes four coronagraphs (Boccaletti et al. 2015) for high-contrast imaging. The four coronagraphs are optimized for observations at 10.65 μm, 11.40 μm, 15.50 μm, and $\sim$23 μm. The short-wavelength coronagraphs use four-quadrant phase masks (4QPM; Rouan et al. 2000, 2007), while the other is a more traditional Lyot design with an occulting spot in the image plane and a stop in the pupil plane. The 4QPMs are usable at a smaller inner working angle than more traditional designs and can reach near $1\lambda/D$. Each of the 4QPMs provides a field of $24'' \times 24''$, while the Lyot spot mask provides $30'' \times 30''$ field of view. Each of the coronagraphs demonstrated a raw contrast ratio >10,000 at $6\lambda/D$ during commissioning. An example that uses this mode can be found in Program 1618, which will search for planets and zodiacal dust around Alpha Centauri A.

6. Science Operations and Proposal Preparation

JWST is controlled from a Mission Operations Center (MOC) at the Space Telescope Science Institute (STScI), which also runs the JWST science program. STScI issues annual calls for proposals (CFPs) for the General Observer programs. Between the CFPs, proposals for time-critical observations or other observations that cannot be proposed to the annual call are considered for the DD time. The scope of JWST's competitively selected programs range from large and Treasury programs that address multiple science goals and produce multi-use data sets to small programs that target important but specific science goals. All of the JWST data taken, including science programs and calibration data, are placed in the Mikulski Archive for Space Telescopes (MAST) at STScI and made available to the original proposers within a day or two of the data being taken. After an exclusive use period that ranges from 0 to 12 months, depending on the type of program, the data are also made freely available to other astronomers for archival research and other purposes.

In response to the annual CFP, proposals are prepared using the Astronomer's Proposal Tool (APT) software package, which allows the proposer to specify both the textual proposal information (e.g., Title, Abstract, investigators, etc.) and the specifics of the observations. The APT is a sophisticated software package that ensures appropriate selection of observing parameters, checks the feasibility of the observations, and determines the times of the year that the observations could be scheduled, including planning guide star availability. APT also calculates the total allocated time needed for the observations. The text of the scientific justification and other proposal sections are attached to the proposal as a PDF within APT.

In addition to APT, observers will use the JWST Exposure Time Calculator (ETC) to determine many of the observation parameters, and to ensure that the observations reach the depth required for the science. The APT and ETC together contain sophisticated data simulation tools to visualize potential JWST observations. APT and the ETC are documented in an extensive series of on-line pages that are known as the JWST User Documentation (JDox, STScI 2016).[89] JDox also documents the JWST data analysis tools.

[89] For more information about proposing for JWST's observing time or archival funding, see: https://jwst-docs.stsci.edu/.

7. Getting JWST to Space: What Might We Find and What's Next?

Building on the inspiring and poetic 1996 HST and Beyond report of the Dressler committee, and with the vigorous support of NASA, ESA, and CSA leadership, the JWST team settled on the four top scientific priorities, documented the instrument and telescope performance requirements to meet scientific objectives, made plans, matured 10 technologies, made international agreements, and chose the instrument teams and contractors. The result is the world's most powerful space telescope, which performs better than expectations, with a projected lifetime of 20 yr. We have reviewed the history, key technical choices, and we celebrate the people who made the observatory real.

We already see progress in the four key science themes. JWST has begun to address questions of the first galaxies and reionization by measuring spectroscopic redshifts of metal-poor galaxies beyond $z > 13$ (Curtis-Lake et al. 2023), detecting multiple emission lines in a galaxy at $z = 10.6$ (Bunker et al. 2023), and measuring galaxy luminosity functions at $z > 7$ (Finkelstein et al. 2023). JWST has studied galaxy assembly by detecting galaxy bars at $z > 1$ (Guo et al. 2023) and examining the quasar-galaxy connection at $z = 2.94$ (Wylezalek 2022). JWST has peered into star-forming regions to study the interactions between massive stars and the surrounding material (Reiter et al. 2022) and measured the ice chemistry in a prestellar cloud (McClure et al. 2023). JWST has measured the temperature of a rocky exoplanet (Greene et al. 2023), and made the first detection of CO_2 in an exoplanet atmosphere (JWST Transiting Exoplanet Community Early Release Science Team et al. 2023). JWST observed the impact of NASA's Double Asteroid Redirection Test (DART) into asteroid Dimorphos and has made a detailed study of the Jovian system (de Pater et al. 2022). Further JWST observations will continue to address the original science themes and it is likely that the universe will surprise us with unexpected discoveries. Looking toward the future, our international teams have proven that extremely complex scientific space missions can be successful, paving the way toward the future great observatories that were recommended by the 2020 Decadal Survey.

Acknowledgments

The JWST mission is a joint project between the National Aeronautics and Space Agency, European Space Agency, and the Canadian Space Agency. The development of the JWST mission was led at NASA's Goddard Space Flight Center with a distributed team across Northrop Grumman Corporation, Ball Aerospace, L3Harris Technologies, the Space Telescope Science Institute, and hundreds of other companies and institutions. This mission was created by a team of people whose creativity and dedication made this scientific dream a reality.

Technical contributions were carried out at the Jet Propulsion Laboratory, California Institute of Technology, under a contract with the National Aeronautics and Space Administration (80NM0018D0004).

This work is based on observations made with the NASA/ESA/CSA James Webb Space Telescope. The data were obtained from the Mikulski Archive for Space Telescopes at the Space Telescope Science Institute, which is operated by the Association of Universities for Research in Astronomy, Inc., under NASA contract NAS 5-03127 for JWST.

ORCID iDs

Jonathan P. Gardner https://orcid.org/0000-0003-2098-9568
John C. Mather https://orcid.org/0000-0002-6460-0078
John G. Abraham https://orcid.org/0000-0001-6559-6616
Roberto Abraham https://orcid.org/0000-0002-4542-921X
Yasin M. Abul-Huda https://orcid.org/0000-0001-5625-4091
Evan Adams https://orcid.org/0000-0001-5490-2518
Maarten Adriaensen https://orcid.org/0000-0003-0026-3129
Jonathan Albert Aguilar https://orcid.org/0000-0003-3184-0873
Loïc Albert https://orcid.org/0000-0003-0475-9375
Stacey Alberts https://orcid.org/0000-0002-8909-8782
Jose Lorenzo Alvarez https://orcid.org/0000-0002-6845-993X
Javier Álvarez-Márquez https://orcid.org/0000-0002-7093-1877
Catarina Alves de Oliveira https://orcid.org/0000-0003-2896-4138
Jay Anderson https://orcid.org/0000-0003-2861-3995
Jonathan W. Arenberg https://orcid.org/0000-0003-1096-5634
Ioannis Argyriou https://orcid.org/0000-0003-2820-1077
Santiago Arribas https://orcid.org/0000-0001-7997-1640
Étienne Artigau https://orcid.org/0000-0003-3506-5667
Jesse Averbukh https://orcid.org/0000-0002-0041-0363
David A. Baran https://orcid.org/0000-0002-1212-4276
Allison Barto https://orcid.org/0000-0003-0604-8673
Pierre Baudoz https://orcid.org/0000-0002-2711-7116
Kathryn Bechtold https://orcid.org/0000-0002-7722-6900
Tracy Beck https://orcid.org/0000-0002-6881-0574
Charles Beichman https://orcid.org/0000-0002-5627-5471
Antoine-Darveau Bernier https://orcid.org/0000-0002-7786-0661
Stephan Birkmann https://orcid.org/0000-0001-7058-1726
Anthony Boccaletti https://orcid.org/0000-0001-9353-2724
Ralph C. Bohlin https://orcid.org/0000-0001-9806-0551
Torsten Böker https://orcid.org/0000-0002-5666-7782
N. Bonaventura https://orcid.org/0000-0001-8470-7094
Patrice Bouchet https://orcid.org/0000-0002-6018-3393
Jeroen Bouwman https://orcid.org/0000-0003-4757-2500
Martha L. Boyer https://orcid.org/0000-0003-4850-9589
Larry D. Bradley https://orcid.org/0000-0002-7908-9284
Gregory R. Brady https://orcid.org/0000-0003-3249-2436
Bernhard R. Brandl https://orcid.org/0000-0001-9737-169X
Stacey N. Bright https://orcid.org/0000-0001-7951-7966
Thomas M. Brown https://orcid.org/0000-0002-1793-9968
Howard A. Bushouse https://orcid.org/0000-0001-6664-7585
Mihai Cara https://orcid.org/0000-0002-9294-6551
S. Charlot https://orcid.org/0000-0003-3458-2275
Pierre Chayer https://orcid.org/0000-0001-7653-0882
Christine H. Chen https://orcid.org/0000-0002-8382-0447
Brian Cherinka https://orcid.org/0000-0002-4289-7923
Knicole D. Colón https://orcid.org/0000-0001-8020-7121
Luis Colina https://orcid.org/0000-0002-9090-4227
Thomas M. Comeau https://orcid.org/0000-0003-2005-9627
Kyle E. Conroy https://orcid.org/0000-0002-5442-8550
Adam R. Contos https://orcid.org/0000-0003-1398-809X
Neil J. Cook https://orcid.org/0000-0003-4166-4121
Rachel Aviva Cooper https://orcid.org/0000-0001-7864-308X
Christophe Cossou https://orcid.org/0000-0001-5350-4796
Alain Coulais https://orcid.org/0000-0001-6492-7719
Misty M. Cracraft https://orcid.org/0000-0002-7698-3002
Guido De Marchi https://orcid.org/0000-0001-7906-3829
Nadezhda M. Dencheva https://orcid.org/0000-0002-5686-9632
Örs Hunor Detre https://orcid.org/0000-0003-0585-4219
Daniel Dicken https://orcid.org/0000-0003-0589-5969
Ewine F. van Dishoeck https://orcid.org/0000-0001-7591-1907
William V. Dixon https://orcid.org/0000-0001-9184-4716
René Doyon https://orcid.org/0000-0001-5485-4675
Paul Eccleston https://orcid.org/0000-0002-3318-7129
Daniel J. Eisenstein https://orcid.org/0000-0002-2929-3121
Michael Engesser https://orcid.org/0000-0003-0209-674X
Néstor Espinoza https://orcid.org/0000-0001-9513-1449
Mireya Etxaluze https://orcid.org/0000-0002-5628-1193
Raymond Fels https://orcid.org/0000-0003-4321-5418
Henry C. Ferguson https://orcid.org/0000-0001-7113-2738
Laura Ferrarese https://orcid.org/0000-0002-8224-1128
Pierre Ferruit https://orcid.org/0000-0001-8895-0606
Joseph Charles Filippazzo https://orcid.org/0000-0002-0201-8306
Nicolas Flagey https://orcid.org/0000-0002-8763-1555
Scott W. Fleming https://orcid.org/0000-0003-0556-027X
Ori D. Fox https://orcid.org/0000-0003-2238-1572
Marijn Franx https://orcid.org/0000-0002-8871-3026
Scott D. Friedman https://orcid.org/0000-0002-6211-1932
Alexander W. Fullerton https://orcid.org/0000-0003-2429-7964
Macarena García Marín https://orcid.org/0000-0003-4801-0489
Danny Gasman https://orcid.org/0000-0002-1257-7742
András Gáspár https://orcid.org/0000-0001-8612-3236
Vincent Geers https://orcid.org/0000-0003-2692-8926
Mario Gennaro https://orcid.org/0000-0002-5581-2896
Giovanna Giardino https://orcid.org/0000-0002-9262-7155
Julien H. Girard https://orcid.org/0000-0001-8627-0404
Alistair Glasse https://orcid.org/0000-0002-2041-2462
Adrian Michael Glauser https://orcid.org/0000-0001-9250-1547
Karl D. Gordon https://orcid.org/0000-0001-5340-6774
Paul Goudfrooij https://orcid.org/0000-0002-5728-1427
Joel David Green https://orcid.org/0000-0003-1665-5709
Gretchen R. Greene https://orcid.org/0000-0002-2302-9442
Thomas P. Greene https://orcid.org/0000-0002-8963-8056
Perry E. Greenfield https://orcid.org/0000-0003-2269-0551
Thomas R. Greve https://orcid.org/0000-0002-2554-1837
Manuel Güdel https://orcid.org/0000-0001-9818-0588
Pierre Guillard https://orcid.org/0000-0002-2421-1350
Kevin Hainline https://orcid.org/0000-0003-4565-8239
Heidi B. Hammel https://orcid.org/0000-0001-8751-3463
Brian Hayden https://orcid.org/0000-0001-9200-8699
Thomas Henning https://orcid.org/0000-0002-1493-300X
Alaina Henry https://orcid.org/0000-0002-6586-4446
Dean C. Hines https://orcid.org/0000-0003-4653-6161
Klaus Hodapp https://orcid.org/0000-0003-0786-2140
Melissa Hoffman https://orcid.org/0000-0003-2523-4631

Sherie T. Holfeltz https://orcid.org/0000-0002-7092-2022
Bryan Jason Holler https://orcid.org/0000-0002-6117-0164
Scott Horner https://orcid.org/0000-0001-9886-6934
Joseph S. Hunkeler https://orcid.org/0000-0003-4989-0289
Garth Illingworth https://orcid.org/0000-0002-8096-2837
Peter Jakobsen https://orcid.org/0000-0002-6780-2441
William Brian Jamieson https://orcid.org/0000-0001-5976-4492
Ray Jayawardhana https://orcid.org/0000-0001-5349-6853
Doug Johnstone https://orcid.org/0000-0002-6773-459X
Olivia C. Jones https://orcid.org/0000-0003-4870-5547
Ian J. Jordan https://orcid.org/0000-0003-2536-0187
Kay Justtanont https://orcid.org/0000-0003-1689-9201
Jason S. Kalirai https://orcid.org/0000-0001-9690-4159
Lisa Kaltenegger https://orcid.org/0000-0002-0436-1802
Jens Kammerer https://orcid.org/0000-0003-2769-0438
Susan A. Kassin https://orcid.org/0000-0002-3838-8093
Patrick Kavanagh https://orcid.org/0000-0001-6872-2358
Sarah Kendrew https://orcid.org/0000-0002-7612-0469
Charles D. Keyes https://orcid.org/0000-0002-4834-369X
Pamela Klaassen https://orcid.org/0000-0001-9443-0463
Anton M. Koekemoer https://orcid.org/0000-0002-6610-2048
Gerard A. Kriss https://orcid.org/0000-0002-2180-8266
Nimisha Kumari https://orcid.org/0000-0002-5320-2568
Álvaro Labiano https://orcid.org/0000-0002-0690-8824
David Lafrenière https://orcid.org/0000-0002-6780-4252
Stephanie Marie LaMassa https://orcid.org/0000-0002-5907-3330
Richard Joseph Lampenfield https://orcid.org/0000-0003-3457-7660
Kirsten Larson https://orcid.org/0000-0003-3917-6460
David R. Law https://orcid.org/0000-0002-9402-186X
Yat-Ning Paul Lee https://orcid.org/0000-0001-9205-9939
Jarron Leisenring https://orcid.org/0000-0002-0834-6140
Nancy A. Levenson https://orcid.org/0000-0003-4209-639X
Nikole Lewis https://orcid.org/0000-0002-8507-1304
Mattia Libralato https://orcid.org/0000-0001-9673-7397
Paul Lightsey https://orcid.org/0000-0001-9185-1393
Pey Lian Lim https://orcid.org/0000-0003-0079-4114
Douglas R. Long https://orcid.org/0000-0002-2508-9211
Knox S. Long https://orcid.org/0000-0002-4134-864X
Marcos López-Caniego https://orcid.org/0000-0003-1016-9283
Jennifer M. Lotz https://orcid.org/0000-0003-3130-5643
Jonathan Lunine https://orcid.org/0000-0003-2279-4131
Nora Lützgendorf https://orcid.org/0000-0002-4034-0080
Richard J. Lynch https://orcid.org/0000-0002-0491-3486
Roberto Maiolino https://orcid.org/0000-0002-4985-3819
Elena Manjavacas https://orcid.org/0000-0003-0192-6887
Anthony Marston https://orcid.org/0000-0001-5788-5258
Peter G. Martin https://orcid.org/0000-0002-5236-3896
Mark J. McCaughrean https://orcid.org/0000-0002-1452-5268
Michael W. McElwain https://orcid.org/0000-0003-0241-8956
Brian McLean https://orcid.org/0000-0002-8058-643X
Margaret Meixner https://orcid.org/0000-0002-0522-3743
Marcio Meléndez https://orcid.org/0000-0001-8485-0325
Michael R. Meyer https://orcid.org/0000-0003-1227-3084
Stefanie N. Milam https://orcid.org/0000-0001-7694-4129
Takahiro Morishita https://orcid.org/0000-0002-8512-1404
Amaya Moro-Martín https://orcid.org/0000-0001-9504-8426
Susan Elizabeth Mullally https://orcid.org/0000-0001-7106-4683
James C. Muzerolle https://orcid.org/0000-0002-5943-1222
Adrian F. Nagle, IV https://orcid.org/0000-0002-7389-5445
Omnarayani Nayak https://orcid.org/0000-0001-6576-6339
Duy Tuong Nguyen https://orcid.org/0000-0002-1534-336X
Bryony Nickson https://orcid.org/0000-0002-9915-1372
Nikolay K. Nikolov https://orcid.org/0000-0002-0627-6951
Alberto Noriega-Crespo https://orcid.org/0000-0002-6296-8960
Joel D. Offenberg https://orcid.org/0000-0003-3834-6384
Patrick Michael Ogle https://orcid.org/0000-0002-3471-981X
Göran Östlin https://orcid.org/0000-0002-3005-1349
O. Justin Otor https://orcid.org/0000-0002-4679-5692
Nathalie N.-Q. Ouellette https://orcid.org/0000-0003-0409-0579
Camilla Pacifici https://orcid.org/0000-0003-4196-0617
Polychronis Patapis https://orcid.org/0000-0001-8718-3732
Tyler Andrew Pauly https://orcid.org/0000-0001-9500-9267
Maria Peña-Guerrero https://orcid.org/0000-0003-2314-3453
Andrew H. Pedder https://orcid.org/0000-0001-5375-4250
Marshall D. Perrin https://orcid.org/0000-0002-3191-8151
Judy L. Pipher https://orcid.org/0000-0002-0628-9605
Rachel Plesha https://orcid.org/0000-0002-2509-3878
Klaus Pontoppidan https://orcid.org/0000-0001-7552-1562
Charles R. Proffitt https://orcid.org/0000-0001-7617-5665
Laurent Pueyo https://orcid.org/0000-0003-3818-408X
Julien Rameau https://orcid.org/0000-0003-0029-0258
Bernard J. Rauscher https://orcid.org/0000-0003-2662-6821
Swara Ravindranath https://orcid.org/0000-0002-5269-6527
Timothy Rawle https://orcid.org/0000-0002-7028-5588
Tom Ray https://orcid.org/0000-0002-2110-1068
Michael Ressler https://orcid.org/0000-0001-5644-8830
Armin W. Rest https://orcid.org/0000-0002-4410-5387
Joel G. Richon https://orcid.org/0000-0002-3876-7149
Michael Ridgaway https://orcid.org/0000-0003-1645-8596
George H. Rieke https://orcid.org/0000-0003-2303-6519
Marcia J. Rieke https://orcid.org/0000-0002-7893-6170
Jane R. Rigby https://orcid.org/0000-0002-7627-6551
Hans-Walter Rix https://orcid.org/0000-0003-4996-9069
Massimo Robberto https://orcid.org/0000-0002-9573-3199
David R. Rodriguez https://orcid.org/0000-0003-1286-5231
Bruno Rodríguez del Pino https://orcid.org/0000-0001-5171-3930
Anthony J. Roman https://orcid.org/0000-0001-5040-8520
Jose J. Rosales https://orcid.org/0000-0001-8407-459X
Jason Rowe https://orcid.org/0000-0002-5904-1865
Neil Rowlands https://orcid.org/0000-0002-1715-7069
Arpita Roy https://orcid.org/0000-0001-8127-5775
Pierre Royer https://orcid.org/0000-0001-9341-2546
Elena Sabbi https://orcid.org/0000-0003-2954-7643
Kailash C. Sahu https://orcid.org/0000-0001-6008-1955
Piyal Samara-Ratna https://orcid.org/0000-0002-7332-2866

B. A. Sargent https://orcid.org/0000-0001-9855-8261
Marcin Sawicki https://orcid.org/0000-0002-7712-7857
Silvia Scheithauer https://orcid.org/0000-0003-4559-0721
Everett Schlawin https://orcid.org/0000-0001-8291-6490
Bryan Shaughnessy https://orcid.org/0000-0001-6493-0029
Richard A. Shaw https://orcid.org/0000-0003-4058-5202
Kartik Sheth https://orcid.org/0000-0002-5496-4118
Hsin-Yi Shih https://orcid.org/0000-0002-6106-349X
Irene Shivaei https://orcid.org/0000-0003-4702-7561
Matthew G. Sienkiewicz https://orcid.org/0000-0003-4392-6981
Anand Sivaramakrishnan https://orcid.org/0000-0003-1251-4124
G. C. Sloan https://orcid.org/0000-0003-4520-1044
Eric P. Smith https://orcid.org/0000-0002-1332-9740
David R. Soderblom https://orcid.org/0000-0002-0322-8161
Sangmo Tony Sohn https://orcid.org/0000-0001-8368-0221
George Sonneborn https://orcid.org/0000-0003-1440-9897
Remi Soummer https://orcid.org/0000-0003-2753-2819
John A. Stansberry https://orcid.org/0000-0003-2434-5225
Massimo Stiavelli https://orcid.org/0000-0001-9935-6047
Amber N. Straughn https://orcid.org/0000-0002-4772-7878
Fengwu Sun https://orcid.org/0000-0002-4622-6617
Benjamin Dale Sunnquist https://orcid.org/0000-0003-3759-8707
Joanna M. Taylor https://orcid.org/0000-0003-4068-5545
Mason Van Tea https://orcid.org/0000-0001-9638-8393
Tea Temim https://orcid.org/0000-0001-7380-3144
Hien D. Tran https://orcid.org/0000-0001-7548-6664
Jason Tumlinson https://orcid.org/0000-0002-7982-412X
Jeff A. Valenti https://orcid.org/0000-0003-3305-6281
Roeland P. Van Der Marel https://orcid.org/0000-0001-7827-7825
Bart Vandenbussche https://orcid.org/0000-0002-1368-3109
Maria Begoña Vila Costas https://orcid.org/0000-0003-3504-1569
Kevin Volk https://orcid.org/0000-0002-3824-8832
Christoffel Waelkens https://orcid.org/0000-0003-0081-7662
Glenn Michael Wahlgren https://orcid.org/0000-0002-6570-4776
Martyn Wells https://orcid.org/0000-0003-3026-2506
Christina C. Williams https://orcid.org/0000-0003-2919-7495
Christopher N. A. Willmer https://orcid.org/0000-0001-9262-9997
Chris J. Willott https://orcid.org/0000-0002-4201-7367
Rogier Windhorst https://orcid.org/0000-0001-8156-6281
Schuyler Wolff https://orcid.org/0000-0002-9977-8255
Gillian S. Wright https://orcid.org/0000-0001-7416-7936
Peter Zeidler https://orcid.org/0000-0002-6091-7924

References

Armus, L., Mazzarella, J. M., Evans, A. S., et al. 2009, PASP, 121, 559
Albert, L., Lafreniere, D., Doyon, R., et al. 2023, arXiv:2306.04572
Armus, L., Lai, T., U, V., et al. 2023, ApJL, 942, L37
Bahcall, J. 1991, The Decade of Discovery in Astronomy and Astrophysics. (Washington, DC: The National Academies Press) Astronomy and Astrophysics Survey Committee
Bakx, T. J. L. C., Zavala, J. A., Mitsuhashi, I., et al. 2023, MNRAS, 519, 5076
Beckwith, S. V. W., Stiavelli, M., Koekemoer, A. M., et al. 2006, AJ, 132, 1729
Bely, P. Y. 2003, The Design and Construction of Large Optical Telescopes (New York: Springer), doi:10.1007/b97612
Bely, P. Y., Burrows, C. J., & Illingworth, G. D. 1990, The Next Generation Space Telescope (Baltimore, MD: Space Telescope Science Institute)
Bentz, M. C., Williams, P. R., & Treu, T. 2022, ApJ, 934, 168
Bergamini, P., Acebron, A., Grillo, C., et al. 2023, A&A, 670, A60
Berné, O., Habart, É., Peeters, E., et al. 2022, PASP, 134, 054301
Birkmann, S. M., Ferruit, P., Giardino, G., et al. 2022, A&A, 661, A83
Boccaletti, A., Lagage, P. O., Baudoz, P., et al. 2015, PASP, 127, 633
Bohn, T., Inami, H., Diaz-Santos, T., et al. 2023, ApJL, 942, L36
Böker, T., Arribas, S., Lützgendorf, N., et al. 2022, A&A, 661, A82
Böker, T., Beck, T. L., Birkmann, S. M., et al. 2023, PASP, 135, 038001
Bouchet, P., García-Marín, M., Lagage, P. O., et al. 2015, PASP, 127, 612
Boyett, K., Mascia, S., Pentericci, L., et al. 2022, ApJL, 940, L52
Bunker, A. J., Saxena, A., Cameron, A. J., et al. 2023, arXiv:2302.07256
Burrows, C. J., Holtzman, J. A., Faber, S. M., et al. 1991, ApJL, 369, L21
Carnall, A. C., McLeod, D. J., McLure, R. J., et al. 2023, MNRAS, 520, 3974
Carter, A. L., Hinkley, S., Kammerer, J., et al. 2022, arXiv:2208.14990
Castellano, M., Fontana, A., Treu, T., et al. 2022, ApJL, 938, L15
Chen, C.-C., Gao, Z.-K., Hsu, Q.-N., et al. 2022a, ApJL, 939, L7
Chen, W., Kelly, P. L., Treu, T., et al. 2022b, ApJL, 940, L54
Chen, Z., Stark, D. P., Endsley, R., et al. 2023, MNRAS, 518, 5607
Curtis-Lake, E., Carniani, S., Cameron, A., et al. 2023, NatAs, 7, 622
de Pater, I., Fouchet, T., Wong, M., et al. 2022, AAS/DPS Meeting Abstracts, 54, 306.07
Ding, X., Silverman, J. D., & Onoue, M. 2022, ApJL, 939, L28
Doyon, R., Hutchings, J. B., Beaulieu, M., et al. 2012, Proc. SPIE, 8442, 84422R
Doyon, R., Willott, C. J., Hutchings, J., et al. 2023, PASP, submitted
Dressler, A. 1996, HST and beyond., Association of Universities for Research in Astronomy (Washington, D.C) HST and Beyond Committee
Dressler, A., Vulcani, B., Treu, T., et al. 2023, ApJL, 947, L27
Espinoza, N., Úbeda, L., Birkmann, S. M., et al. 2023, PASP, 135, 018002
Evans, A. S., Frayer, D., Charmandaris, V., et al. 2022, ApJL, 940, L8
Feinberg, L. D., Clampin, M., Keski-Kuha, R., et al. 2012, Proc. SPIE, 8442, 84422B
Ferruit, P., Jakobsen, P., Giardino, G., et al. 2022, A&A, 661, A81
Field, G. B. 1983, Astronomy and Astrophysics Survey Committee, Vol. 1 (Washington, DC: The National Academies Press)
Fienup, J. R., Marron, J. C., Schulz, T. J., & Seldin, J. H. 1993, ApOpt, 32, 1747
Finkelstein, S. L., Bagley, M. B., Arrabal Haro, P., et al. 2022, ApJL, 940, L55
Finkelstein, S. L., Bagley, M. B., Ferguson, H. C., et al. 2023, ApJL, 946, L13
Freedman, W. L., Madore, B. F., Gibson, B. K., et al. 2001, ApJ, 553, 47
Gaia Collaboration, Brown, A. G. A., Vallenari, A., et al. 2018, A&A, 616, A1
Gardner, J. P., Cowie, L. L., & Wainscoat, R. J. 1993, ApJL, 415, L9
Gardner, J. P., Mather, J. C., Clampin, M., et al. 2006, SSRv, 123, 485
Gardner, J. P., & Satyapal, S. 2000, AJ, 119, 2589
Giavalisco, M., Ferguson, H. C., Koekemoer, A. M., et al. 2004, ApJL, 600, L93
Gilbert, K., Weisz, D. & Resolved Stellar Populations ERS Program Team 2018, AAS Meeting Abstracts, 232, 210.02
Girard, J. H., Leisenring, J., Kammerer, J., et al. 2022, Proc. SPIE, 12180, 121803Q
Glasse, A., Rieke, G. H., Bauwens, E., et al. 2015, PASP, 127, 686
Glazebrook, K., Nanayakkara, T., Jacobs, C., et al. 2023, ApJL, 947, L25
Greene, T. P., Bell, T. J., Ducrot, E., et al. 2023, Natur, 618, 39
Greene, T. P., Kelly, D. M., Stansberry, J., et al. 2017, JATIS, 3, 035001
Greenhouse, M. 2016, Proc. SPIE, 9904, 990406
Grogin, N. A., Kocevski, D. D., Faber, S. M., et al. 2011, ApJS, 197, 35
Guo, Y., Jogee, S., Finkelstein, S. L., et al. 2023, ApJL, 945, L10
Hinkley, S., Carter, A. L., Ray, S., et al. 2022, PASP, 134, 095003
Horner, S. D., & Rieke, M. J. 2004, Proc. SPIE, 5487, 628
Illingworth, G. 1991, JPL D-8541, Technologies for Large Filled Aperture Telescopes in Space, Vol. 4 (Pasadena, CA: JPL)
Inami, H., Surace, J., Armus, L., et al. 2022, ApJL, 940, L6
Jacobs, C., Glazebrook, K., Calabrò, A., et al. 2023, ApJL, 948, L13
Jakobsen, P., Ferruit, P., Alves de Oliveira, C., et al. 2022, A&A, 661, A80
JWST Transiting Exoplanet Community Early Release Science Team, Ahrer, E.-M., Alderson, L., et al. 2023, Natur, 614, 649
Kaldeich-Schürmann, B. 1998, ESA Special Publication, The Next Generation Space Telescope: Science Drivers and Technological Challenges, Vol. 429 (Noordwijk: ESA)

Kammerer, J., Girard, J., Carter, A. L., et al. 2022, Proc. SPIE, 12180, 121803N
Kendrew, S., Scheithauer, S., Bouchet, P., et al. 2015, PASP, 127, 623
Kimble, R. A., Feinberg, L. D., Voyton, M. F., et al. 2018, Proc. SPIE, 10698, 1069805
Kimble, R. A., Vila, M. B., Van Campen, J. M., et al. 2016, Proc. SPIE, 9904, 990408
Kocevski, D. D., Barro, G., McGrath, E. J., et al. 2023, ApJL, 946, L14
Koekemoer, A. M., Faber, S. M., Ferguson, H. C., et al. 2011, ApJS, 197, 36
Krist, J. E., Balasubramanian, K., Beichman, C. A., et al. 2009, Proc. SPIE, 7440, 74400W
Krist, J. E., & Burrows, C. J. 1995, ApOpt, 34, 4951
Lai, T. S.-Y., Armus, L., U, V., et al. 2022, ApJL, 941, L36
Lambright, W. H. 1995, Powering Apollo: James E. Webb of NASA (Baltimore, MD: John Hopkins Univ. Press)
Lau, R. M. & WR DustERS Team 2022, in IR2022 (An Infrared Bright Future for Ground-based IR Observatories in the Era of JWST)
Lau, R. M., Eldridge, J. J., Hankins, M. J., et al. 2020, ApJ, 898, 74
Leethochawalit, N., Trenti, M., Santini, P., et al. 2022, arXiv:2207.11135
Levenson, N. A., & Sembach, K. 2018, AAS Meeting Abstracts, 232, 202.01
Lotz, J. M., Koekemoer, A., Coe, D., et al. 2017, ApJ, 837, 97
MacKenty, J. W., & Stiavelli, M. 2000, in ASP Conf. Ser. 195, Imaging the Universe in Three Dimensions, ed. W. van Breugel & J. Bland-Hawthorn (San Francisco, CA: ASP), 443
Marchesini, D., Brammer, G., Morishita, T., et al. 2023, ApJL, 942, L25
Mather, J. C., Cheng, E. S., Cottingham, D. A., et al. 1994, ApJ, 420, 439
Mather, J. C., & Stockman, H. S. 2000, Proc. SPIE, 4013, 2
McClure, M. 2022, in 44th COSPAR Scientific Assembly, 2798, published online
McClure, M. K., Boogert, A., Linnartz, H., et al. 2018, AAS Meeting Abstracts, 232, 302.03
McClure, M. K., Rocha, W. R. M., Pontoppidan, K. M., et al. 2023, NatAs, 7, 431
McElwain, M. W., Feinberg, L. D., Perrin, M. D., et al. 2023, PASP, 135, 058001
McKee, C. F., & Taylor, J. H. 2001, Astronomy and Astrophysics in the New Millennium (Washington, DC: The National Academies Press) Astronomy and Astrophysics Survey Committee, doi:10.17226/9839
Menzel, M., Davis, M., Parrish, K., et al. 2023, PASP, in press
Merlin, E., Bonchi, A., Paris, D., et al. 2022, ApJL, 938, L14
Miles, B. E., Biller, B. A., Patapis, P., et al. 2023, ApJL, 946, L6
Moseley, S. H., Fettig, R. K., Kutyrev, A. S., et al. 1999, Proc. SPIE, 3878, 392
Naidu, R. P., Oesch, P. A., van Dokkum, P., et al. 2022, ApJL, 940, L14
Nanayakkara, T., Glazebrook, K., Jacobs, C., et al. 2023, ApJL, 947, L26
Nardiello, D., Bedin, L. R., Burgasser, A., et al. 2022, MNRAS, 517, 484
National Academies of Sciences, E., & Medicine 2021, Pathways to Discovery in Astronomy and Astrophysics for the 2020s
Nonino, M., Glazebrook, K., Burgasser, A. J., et al. 2023, ApJL, 942, L29
Ono, Y., Harikane, Y., Ouchi, M., et al. 2022, arXiv:2208.13582
Onoue, M., Inayoshi, K., Ding, X., et al. 2023, ApJL, 942, L17
Perlmutter, S., Aldering, G., Goldhaber, G., et al. 1999, ApJ, 517, 565
Pontoppidan, K. M., Barrientes, J., Blome, C., et al. 2022, ApJL, 936, L14
Popping, G. 2023, A&A, 669, L8
Rauscher, B. J. 2014, AAS Meeting Abstracts, 223, 149.39
Rauscher, B. J., Boehm, N., Cagiano, S., et al. 2014, PASP, 126, 739
Reiter, M., Morse, J. A., Smith, N., et al. 2022, MNRAS, 517, 5382
Ressler, M. E., Sukhatme, K. G., Franklin, B. R., et al. 2015, PASP, 127, 675
Rieke, G. H., Ressler, M. E., Morrison, J. E., et al. 2015b, PASP, 127, 665
Rieke, G. H., Wright, G. S., Böker, T., et al. 2015a, PASP, 127, 584
Rieke, M. J., Baum, S. A., Beichman, C. A., et al. 2003, Proc. SPIE, 4850, 478
Rieke, M. J., Kelly, D. M., Misselt, K., et al. 2023, PASP, 135, 028001
Riess, A. G., Filippenko, A. V., Challis, P., et al. 1998, AJ, 116, 1009
Rigby, J. & Templates Team 2020, AAS Meeting Abstracts, 235, 208.12
Rigby, J., Perrin, M., McElwain, M., et al. 2023a, PASP, 135, 048001
Rigby, J. R., Lightsey, P. A., García Marín, M., et al. 2023b, PASP, 135, 048002
Roberts-Borsani, G., Morishita, T., Treu, T., et al. 2022, ApJL, 938, L13
Rouan, D., Baudrand, J., Boccaletti, A., et al. 2007, CRPhy, 8, 298
Rouan, D., Riaud, P., Boccaletti, A., Clénet, Y., & Labeyrie, A. 2000, PASP, 112, 1479
Santini, P., Fontana, A., Castellano, M., et al. 2023, ApJL, 942, L27
Schmidt, B. P., Suntzeff, N. B., Phillips, M. M., et al. 1998, ApJ, 507, 46
Sivaramakrishnan, A., Lafrenière, D., Ford, K. E. S., et al. 2012, Proc. SPIE, 8442, 84422S
Sivaramakrishnan, A., Tuthill, P., Lloyd, J. P., et al. 2023, PASP, 135, 015003
Smith, E. P., & Koratkar, A. 1998, in ASP Conf. Ser. 133, Science With The NGST (Next Generation of Space Telescope) (San Francisco, CA: ASP)
Smith, E. P., & Long, K. S. 2000, in ASP Conf. Ser. 207, Next Generation Space Telescope Science and Technology (San Francisco, CA: ASP)
Stahl, H. P., Feinberg, L. D., & Texter, S. C. 2004, Proc. SPIE, 5487, 818
Stockman, H. S. 1997, The Next Generation Space Telescope. Visiting a time when galaxies were young (Baltimore, MD: The Association of Universities for Research in Astronomy)
Stockman, H. S., & Mather, J. C. 2001, in IAU Symp. 204, (The Extragalactic Infrared Background and its Cosmological Implications) ed. M. Harwit & M. G. Hauser (Cambridge: Cambridge Univ. Press), 467
STScI 2016, JWST User Documentation (JDox), JWST User Documentation Website
Sun, F., Egami, E., Pirzkal, N., et al. 2022a, ApJL, 936, L8
Sun, F., Egami, E., Pirzkal, N., et al. 2022b, arXiv:2209.03374
Thronson, H. A., Hawarden, T. G., Davies, J. K., et al. 1996, AdSpR, 18, 171
Topping, M. W., Stark, D. P., Endsley, R., et al. 2022, ApJ, 941, 153
Treu, T., Roberts-Borsani, G., Bradac, M., et al. 2022, ApJ, 935, 110
Treu, T., Calabro, A., Castellano, M., et al. 2023, ApJL, 942, L28
U, V., Lai, T., Bianchin, M., et al. 2022, ApJL, 940, L5
Vanzella, E., Castellano, M., Bergamini, P., et al. 2022, ApJL, 940, L53
Wade, L. A., Lilienthal, G. W., Terebey, S., et al. 1996, Proc. SPIE, 2807, 20
Wang, X., Jones, T., Vulcani, B., et al. 2022, ApJL, 938, L16
Warfield, J. T., Richstein, H., Kallivayalil, N., et al. 2023, RNAAS, 7, 23
Weisz, D. R., McQuinn, K. B. W., Savino, A., et al. 2023, arXiv:2301.04659
Wells, M., Pel, J. W., Glasse, A., et al. 2015, PASP, 127, 646
Werner, M. W., Roellig, T. L., Low, F. J., et al. 2004, ApJS, 154, 1
Williams, R. E., Blacker, B., Dickinson, M., et al. 1996, AJ, 112, 1335
Willott, C. J., Doyon, R., Albert, L., et al. 2022, PASP, 134, 025002
Wright, G., Rieke, G., Glasse, A., et al. 2023, PASP, 135, 048003
Wright, G. S., Wright, D., Goodson, G. B., et al. 2015, PASP, 127, 595
Wylezalek, D. 2022, Multiphase AGN Feeding & Feedback II, 75
Yang, L., Morishita, T., Leethochawalit, N., et al. 2022, ApJL, 938, L17